



UNIVERSITÀ DI PARMA

ARCHIVIO DELLA RICERCA

University of Parma Research Repository

Impact of PRRSV strains of different in vivo virulence on the macrophage population of the thymus

This is the peer reviewed version of the following article:

Original

Impact of PRRSV strains of different in vivo virulence on the macrophage population of the thymus / Ogno, Giulia; Rodríguez-Gómez, Irene M.; Canelli, Elena; Ruedas-Torres, Inés; Álvarez, Belén; Domínguez, Javier; Borghetti, Paolo; Martelli, Paolo; Gómez-Laguna, Jaime. - In: VETERINARY MICROBIOLOGY. - ISSN 0378-1135. - 232:(2019), pp. 137-145. [10.1016/j.vetmic.2019.04.016]

Availability:

This version is available at: 11381/2859023 since: 2021-10-08T08:47:17Z

Publisher:

Elsevier B.V.

Published

DOI:10.1016/j.vetmic.2019.04.016

Terms of use:

Anyone can freely access the full text of works made available as "Open Access". Works made available

Publisher copyright

note finali coverpage

(Article begins on next page)

02 May 2026

Manuscript Details

Manuscript number	VETMIC_2019_45_R1
Title	Impact of PRRSV strains of different in vivo virulence on the macrophage population of the thymus
Article type	Research Paper

Abstract

The emergence of “highly pathogenic” isolates of porcine reproductive and respiratory syndrome virus (HP-PRRSV) has raised new concerns about PRRS control. Cells from the porcine monocyte-macrophage lineage represent the target for this virus, which replicates mainly in the lung, and especially in HP-PRRSV strains, also in lymphoid organs, such as the thymus. This study aimed at evaluating the impact of two PRRSV strains of different virulence on thymic macrophages as well as after heterologous vaccination. After experimental infection with PR11 and PR40 PRRSV1 subtype 1 strains (low and high virulent, respectively) samples from thymus were analysed by histopathology and immunohistochemistry for PRRSV N protein, TUNEL, CD172a, CD163, CD107a and BA4D5 expression. Mortality was similar in both infected groups, but lung lesions and thymus atrophy were more intense in PR40 group. Animals died at 10-14 dpi after PR11 or PR40 infection showed the most severe histopathological lesions, with a strong inflammatory response of the stroma and extensive cell death phenomena in the cortex. These animals presented an increase in the number of N protein, CD172a, CD163 and BA4D5 positive cells in the stroma and the cortex together with a decrease in the number of CD107a positive cells. Our results highlight the recruitment of macrophages in the thymus, the increase in the expression of CD163 and the regulation of the host cytotoxic activity by macrophages. However, no marked differences were observed between PR11- and PR40-infected animals. Heterologous vaccination restrained virus spread and lesions extent in the thymus of PR40-infected animals.

Keywords virulence; PRRSV; macrophages; thymus; cell death

Manuscript category Viruses

Corresponding Author Jaime Gómez-Laguna

Corresponding Author's Institution Faculty of Veterinary Medicine. University of Córdoba

Order of Authors Giulia Ogno, Irene Magdalena Rodríguez-Gómez, ELENA CANELLI, Inés Ruedas-Torres, Belén Álvarez, Javier Dominguez, Paolo Borghetti, Paolo Martelli, Jaime Gómez-Laguna

Submission Files Included in this PDF

File Name [File Type]

Covert Letter_R1.doc.docx [Cover Letter]

Answer to Reviewer comments.docx [Response to Reviewers]

Revised manuscript with changes marked_R1_Ogno et al.docx [Revised Manuscript with Changes Marked]

Highlights.docx [Highlights]

Manuscript_R1_Ogno et al.docx [Manuscript File]

Figure1.pdf [Figure]

Figure 2.tif [Figure]

Figure 3.tif [Figure]

Figure 4.tif [Figure]

Figure 5.tif [Figure]

To view all the submission files, including those not included in the PDF, click on the manuscript title on your EVISE Homepage, then click 'Download zip file'.



Facultad de Veterinaria
Universidad de Córdoba

Jaime Gómez-Laguna, DVM, MSc, PhD
Department of Anatomy and Comparative Pathology
Faculty of Veterinary Medicine, University of Córdoba
International Excellence Agrifood Campus 'ceiA3'
Córdoba (SPAIN)
Email: y92golaj@uco.es

Dear Dr. V. von Messling
Editor in Chief
Veterinary Microbiology

25th March, 2019
Córdoba, Spain

Dear Editor,

Enclosed you will find the revised version of our original manuscript entitled: “Impact of PRRSV strains of different *in vivo* virulence on the macrophage population of the thymus”, to be considered for its publication in Veterinary Microbiology.

We believe that our manuscript has been now substantially improved taking into account the reviewer's comments. Thus, we hope that the new version of the manuscript is suitable for publication in Veterinary Microbiology. All the authors have seen and approved the revised version of the manuscript.

Yours sincerely,

Jaime Gómez-Laguna, DVM, MSc, PhD

Ref: VETMIC_2019_45

Title: Impact of PRRSV strains of different in vivo virulence on the macrophage population of the thymus

Journal: Veterinary Microbiology

Answers to reviewer's comments

The taxonomy of PRRSV has been changed again according to the latest ratification of the ICTV committee in October 2018. https://talk.ictvonline.org/taxonomy/p/taxonomy-history?taxnode_id=20186087 The current classification refers to PRRSV-1 as Betaarterivirus suid 1 (Nidovirales - Arnidovirineae - Arteriviridae - Variarterivirinae - Betaarterivirus - Eurpobartevirus and Ampobarterivirus), change the text accordingly, to reflect the latest nomenclature, at least the Betaarterivirus genus. There are recent, comprehensive papers available from 2018 regarding PRRSV-1 phylogeny, please refer to those.

The taxonomy of PRRSV has been updated within the manuscript according to the information given by the reviewer. In addition, a new reference has been included to support the diversity in PRRSV1 phylogeny as suggested.

When describing HP strains of PRRSV an entire paragraph could be added regarding HP PRRSV-1 strains and history, including those of subtype 2 (LENA and SU-1bel) and even those of subtype 1 (13V092 in Belgium, Frydas et al 2013; and ACRO in Austria Sinn et al. 2016).

We have added a new phrase with information about the identification of virulent strains within the different subtypes from PRRSV1 (Lines 59-63). In addition, a sentence regarding the clinical signs determined by virulent PRRSV strains has been included in Lines 82-84. We would like to highlight, that with these new changes the length of the Introduction is a little bit over the limit prefixed in the "Guide for the authors" for this journal (not exceed from 2 manuscript pages).

In lines 86-87 (now, lines 96-97), when describing the role of CD163, I suggest to refer first to Calvert et al 2007 (J. Virol), as they were the first group to highlight the role of CD163, then include the groundbreaking papers of Whithworth et al 2015, and Burkard et al 2017 describing the importance of full KO or SRCRD5 deleted CD163 in PRRSV infection, respectively.

The new references have been included as well as a short sentence with the main findings from Whithworth et al., 2015, and Burkard et al., 2017.

In the materials and methods part it would be useful to get more information about the INIA in house mAbs in order to increase the reproducibility of the paper. A few sentences about the method of their generation.

These mAbs have been extensively used and reported in the literature. Accordingly, a brief paragraph has been added to explain how were the hybridomas produced and the corresponding references have been also included (Lines 176-181).

Lines 179-180. If the authors have gross picture regarding the "complete atrophy" of the cervical part of the thymus please include it along with a control organ, as it would look very informative.

Regrettably, we do not have any representative gross picture of the almost complete thymus atrophy in the PR0 group to be included in the manuscript.

Line 182. Rephrase the sentence as in its present form it sounds like the animals were infected with both viruses at the same time.

This sentence has been accordingly modified to avoid misunderstanding.

Line 190. Perivascular area should be used instead of "level".

This change has been accomplished as suggested by the reviewer's comment.

Lines 207-208 and lines 308-309. "TUNEL positive cells were mainly found in tingible body macrophages" A bit of explanation is needed or rephrase this sentence in the discussion. Does this mean that the tingible body macrophages are apoptotic themselves or they contain TUNEL positive fragments that are not yet fully degraded?

Both sentences regarding the TUNEL labelling have been modified to clarify that the staining was observed both in cellular fragments phagocytised by tingible body macrophages as well as in apoptotic bodies.

Line 338. Refer to CD163 knock out animals as indicated for the introduction.

The reference has been accordingly included.

Line 340. Philippidis et al., 2004 has a different font, not TNR.

The font of the reference has been modified.

Figures:

Fig 2B – maybe an asterisk could mark the Hassal's corpuscle similarly to C

According to reviewer's comment two arrows have been included in Fig. 2B to better identify the Hassal's corpuscle

Fig 4 - In case of C and maybe even D the level of magnification is not sufficient to observe the positive cells, I suggest to use the same magnification as for 2 B and C

New figures at higher magnifications have been included for Fig. 4C and 4D to allow an easier identification of positive cells.

Fig 5 - D is hardly visible maybe a single brown dot can be seen nothing else, increase magnification, maybe along with C making all three IHC figures look more uniform

According to reviewer's comment new figures at higher magnifications have been included for Fig. 5C, 5D and 5E.

1 **Impact of PRRSV strains of different *in vivo* virulence on the macrophage population of the**
2 **thymus**

3

4 Giulia Ognò^a, Irene M. Rodríguez-Gómez^b, Elena Canelli^a, Inés Ruedas-Torres^b, Belén Álvarez^c,
5 Javier Domínguez^c, Paolo Borghetti^a, Paolo Martelli^{a,1}, Jaime Gómez-Laguna^{b,1,*}

6

7

8 ^a Department of Veterinary Science, University of Parma, Strada del Taglio, Parma, 10 – 43126,
9 Italy.

10 ^b Department of Anatomy and Comparative Pathology, Faculty of Veterinary Medicine, University
11 of Cordoba, International Excellence Agrifood Campus ‘ceiA3’, Córdoba, Spain.

12 ^c Department of Biotechnology, National Institute for Agricultural and Food Research and
13 Technology (INIA), Madrid, Spain.

14

15 ¹Both authors contributed equally as last authors

16

17

18 ***Corresponding author at:** Department of Anatomy and Comparative Pathology, Faculty of
19 Veterinary Medicine, University of Córdoba, 14071, Córdoba, Spain.

20 Tel.: +34 957 218 162. Fax: +34 057 218 682. Email: v92golaj@uco.es (J. Gómez-Laguna)

21 **Abstract**

22 The emergence of “highly pathogenic” isolates of porcine reproductive and respiratory syndrome
23 virus (HP-PRRSV) has raised new concerns about PRRS control. Cells from the porcine monocyte-
24 macrophage lineage represent the target for this virus, which replicates mainly in the lung, and
25 especially in HP-PRRSV strains, also in lymphoid organs, such as the thymus. This study aimed at
26 evaluating the impact of two PRRSV strains of different virulence on thymic macrophages as well
27 as after heterologous vaccination. After experimental infection with PR11 and PR40 PRRSV1
28 subtype 1 strains (low and high virulent, respectively) samples from thymus were analysed by
29 histopathology and immunohistochemistry for PRRSV N protein, TUNEL, CD172a, CD163,
30 CD107a and BA4D5 expression. Mortality was similar in both infected groups, but lung lesions and
31 thymus atrophy were more intense in PR40 group. Animals died at 10-14 dpi after PR11 or PR40
32 infection showed the most severe histopathological lesions, with a strong inflammatory response of
33 the stroma and extensive cell death phenomena in the cortex. These animals presented an increase
34 in the number of N protein, CD172a, CD163 and BA4D5 positive cells in the stroma and the cortex
35 together with a decrease in the number of CD107a positive cells. Our results highlight the
36 recruitment of macrophages in the thymus, the increase in the expression of CD163 and the
37 regulation of the host cytotoxic activity by macrophages. However, no marked differences were
38 observed between PR11- and PR40-infected animals. Heterologous vaccination restrained virus
39 spread and lesions extent in the thymus of PR40-infected animals.

40

41 *Keywords:* virulence; PRRSV; macrophages; thymus; cell death.

42 1. Introduction

43 Porcine reproductive and respiratory syndrome virus (PRRSV) is a major swine pathogen that
44 induces severe respiratory symptoms in growing and finishing pigs and reproductive failure in gilts
45 and sows, causing considerable economic losses worldwide. The genome, of approximately 15 kb
46 in length, consists of a positive-stranded RNA and contains 11 open reading frames (ORFs), coding
47 for structural and non-structural proteins, which are subject to insertions and deletions determining
48 the genetic diversity of the virus (Murtaugh et al., 2010). Recently, the two genotypes of the virus,
49 type 1 or PRRSV1 (European) and type 2 or PRRSV2 (North American), have been included as
50 different viral species within the genus *Betaarterivirus*, particularly *Betaarterivirus suid 1 species for*
51 *PRRSV1 and Betaarterivirus suid 2 species for the PRRSV2, respectively (Gorbalenya et al.,*
52 *2018). Porarterivirus (Adams et al., 2017).* Both viruses present high internal variability, with
53 PRRSV1 being divided into at least four subtypes (pan-European subtype 1, encompassing different
54 lineages, and East European subtypes 2, 3 and 4) and PRRSV2 into at least nine lineages (Nelsen et
55 al., 1999; Stadejek, et al. 2006, 2013; Balka et al., 2018). During the last decade, virulent variants of
56 the virus, referred to as highly pathogenic (HP), have emerged within both PRRSV1 and PRRSV2
57 (Lunney et al., 2010). These virulent strains often result in severe clinical signs, higher mortality
58 rates and higher tropism and viral load in blood and tissues than low virulent PRRSV strains (Tian
59 et al., 2007; Karnyichuk et al., 2010; Canelli et al., 2017). Although virulent PRRSV1 strains have
60 been traditionally associated to subtype 3 strains (Lena and SU1-bel strains), strains with similar
61 characteristics have been identified within subtypes 1 (13V091, AUT15-33 and PR40/2014 strain)
62 and 2 (BOR59 strain) (Karnyichuk et al., 2010; Morgan et al., 2013; Frydas et al., 2015; Sinn et al.,
63 2016; Canelli et al., 2017; Stadejek et al., 2017).

64
65 The efficacy of modified live virus (MLV) vaccines (PRRSV1 and PRRSV2) have been recently
66 tested in challenge trials with virulent isolates (Trus et al., 2014; Do et al., 2015; Bonckaert et al.,
67 2016; Canelli et al., 2018). Partial cross-protection of these vaccines against virulent strains has

68 been reported under experimental conditions with a reduction of the viremia, the severity of clinical
69 signs and lesions, and the duration of the clinical phase. Nevertheless, none of the tested vaccines
70 was able to prevent the transplacental transmission or the respiratory infection.

71

72 The main cell target for PRRSV replication is the pulmonary alveolar macrophage (PAM) but viral
73 replication has been also widely reported in other macrophage subpopulations from lungs as well as
74 from lymphoid organs of infected animals (Duan et al., 1997; Gómez-Laguna et al., 2010; Barranco
75 et al., 2012). Among lymphoid organs, the thymus particularly plays a central role in the
76 development of the immune system through the differentiation and maturation of T cells (Pearse et
77 al., 2006b). PRRSV infection is characterised by an immunosuppression state associated with,
78 among other factors, atrophy of the thymus and a major decrease in the number of thymocytes in
79 the cortex with marked differences according to the virulence of the PRRSV strain (Amarilla et al.,
80 2016). Thus, so-called HP-PRRSV strains cause more severe clinical signs, long-lasting viremia,
81 higher virus level in blood and tissues, and higher frequency of mortality (Lunney et al., 2010);
82 moreover, these strains predispose piglets to weak cellular immunity together with thymus atrophy,
83 T cell depletion and impairment of the development of naïve T cells (Han et al., 2017).

84

85 In a general context, macrophages perform three main functions: antigen presentation, phagocytosis
86 and synthesis and secretion of cytokines (Geissman et al., 2010). However, the whole range of
87 functions of thymic macrophages is still nowadays unclear. The macrophage population in the
88 thymus is evenly distributed in the cortex and in the medulla and is particularly designated, at least,
89 to phagocytose and remove apoptotic bodies and self-reactive lymphocytes as well as to release
90 mediators involved in thymocytes maturation (Pearse et al., 2006a). As a myeloid cell, the main
91 macrophage marker extensively used is CD172a, which is strongly expressed from the early stages
92 of differentiation onwards (Summerfield et al., 1997). A restricted marker to monocyte and
93 macrophages is CD163, a member of the family of proteins with scavenger receptor cysteine-rich

94 domains (Law et al., 1993). Particularly, CD163 has been identified to be the major receptor for
95 PRRSV uncoating and genome release ([Calvert et al., 2007](#); Van Breedam et al., 2010), with well
96 described effects of the deletion of its SRCR5 domain on PRRSV infection ([Whithworth et al.,](#)
97 [2016](#); [Burkard et al., 2017](#)). CD107a, or lysosomal-associated membrane protein 1 (LAMP-1),
98 despite not being restricted to macrophages, has been demonstrated to be useful for identifying
99 macrophages populations in tissue sections, especially, tingible body macrophages in lymphoid
100 organs as well as macrophages from the thymus cortex and medulla (Bullido et al., 1997;
101 Domenech et al., 2003). An interesting marker with a restricted expression for the macrophage
102 lineage is the antigen recognized by the monoclonal antibody BA4D5, which shows features that
103 resemble those of CD68. Thus, this molecule/antigen presents a predominant intracellular location
104 in phagolysosomes with a low expression on the cell surface and has been detected on macrophages
105 from the thymus cortex as well as on other macrophages from spleen and lymph nodes (Ezquerria et
106 al., 2009).

107

108 Considering the role of macrophages in PRRSV replication and on the onset of the host immune
109 response, the impact of two Italian subtype 1 PRRSV1 strains (PR40/2014 and PR11/2014), with
110 different *in vivo* virulence (Canelli et al., 2017), was evaluated in this study. In addition, the effect
111 of a heterologous vaccination on histopathological lesions as well as on macrophages populations of
112 the thymus of HP-PRRSV infected animals was examined.

113

114 **2. Materials and Methods**

115 *2.1. Animals and experimental infection*

116 The *in vivo* study is part of a large project carried out to investigate the pathogenesis and control of
117 PRRSV1 strains of differing virulence; materials analysed in the present study were collected from
118 experiments published elsewhere (Canelli et al., 2017, 2018). Briefly, a total of twelve 4-week-old
119 conventional pigs were assigned to three different experimental groups, as described in Canelli et

120 al. (2017): (i) PR40 group (PR40), with 5 pigs inoculated intra-nasally (IN) with 2 ml, containing
121 10^5 TCD₅₀ of PRRSV1 PR40/2014, per pig; (ii) PR11 group (PR11), with 4 piglets inoculated IN
122 with 2 ml, containing 10^5 TCD₅₀ of PRRSV1 PR11/2014, per pig; and, (iii) Control group (C), with
123 3 animals inoculated IN with sterile medium (mock/negative control). In addition, two different
124 vaccinated groups, described in Canelli et al. (2018), were included: (i) VAC-C: 2 pigs were IM-
125 vaccinated against PRRSV at 4 weeks of age (Porcilis® PRRS, MSD Animal Health; DV strain;
126 vaccine batch A208AD01) and left uninfected; (ii) VAC-PR40: 6 pigs were IM-vaccinated against
127 PRRSV and IN infected with PR40 at 35 days post-vaccination (dpv) (day 0 post-inoculation, dpi)
128 (Fig. 1).

129

130 No relevant pathogens (PRRSV, SIV, PCV2) were detected in the animals before the beginning of
131 the studies. Animals suffering from severe clinical signs with a fatal prognosis were humanely
132 euthanized according to standard protocols. All the survivors were humanely euthanized at 35 dpi
133 (end of the experiment). At necropsy gross pathology was recorded and thymus samples were
134 collected and fixed in buffered-formalin pH 7.4 for histopathology and immunohistochemical
135 studies. The experimental design and all the procedures were fully in agreement and approved by
136 the Ethical Committee and by the Ministry of Health in Italy according to European and National
137 rules on experimental infection studies and animal welfare.

138

139 *2.2. Histopathology and grading of thymus*

140 Four μm tissue sections were stained with haematoxylin and eosin (H&E). The severity of the
141 lesions in thymus was scored as follows (adapted and modified from Amarilla et al., 2016): (i)
142 Grade 0, the cortex:medulla ratio (C/M) is about 2:1 with typical histological characteristics of the
143 thymus; (ii) Grade I, diffuse cortical reduction with focal cortical disappearance, 5–9 tingible body
144 macrophages/mm² within the thymic cortex, typical medulla and stroma; (iii) Grade II, focal or
145 multifocal decrease of C/M (<2:1), decrease of cortical layer with slight proportional increase of the

146 stroma and 10–15 tingible body macrophages/mm² within the thymic cortex; (iv) Grade III, focal to
147 multifocal blurring of normal corticomedullary demarcation, increase of the stroma, occasional
148 increase in the number of lymphocytes, mast and plasma cells and ≥ 16 tingible body
149 macrophages/mm², with a “starry sky” appearance of the tissue; and, (v) Grade IV, extensive cell
150 death of cortical thymocytes with complete disappearance of corticomedullary boundary
151 demarcation and increase of the stroma.

152

153 Manual quantification of tingible body macrophages in thymic cortex was assessed in 25 non-
154 overlapping, consecutively selected high magnification fields of 0.2 mm². Results were expressed
155 as number of cells per mm².

156

157 *2.3. Immunohistochemistry*

158 The Avidin–Biotin–Peroxidase complex technique (ABC Vector Elite, Vector laboratories, USA)
159 was used for the immunolabelling of PRRSV antigen and the different macrophages markers.
160 Terminal dUTP Nick End-Labeling (TUNEL) was carried out by using a commercial kit (In Situ
161 Cell Death Detection Kit, POD, Roche, Germany) following manufacturer’s instructions. Briefly, 4
162 μm tissue sections were dewaxed and rehydrated in a gradient of ethanol, followed by endogenous
163 peroxidase inhibition with 3 % H₂O₂ solution in methanol for 30 minutes (min). After treatment
164 with different antigen retrieval methods (Table 1), the slides were washed with PBS (pH 7.4) and
165 incubated for 30 min at room temperature with 100 μl of blocking solution in a humid chamber.
166 Primary antibodies were incubated overnight at 4 °C in a humid chamber (see dilutions in Table 1
167 for each antibody), while for the negative controls the primary antibody was replaced by either an
168 isotype control or by blocking solution. Biotinylated secondary antibody was incubated for 30 min
169 at room temperature. An avidin-biotin-peroxidase complex (Vector Laboratories) was applied for
170 1 hour at room temperature in the darkness. Labelling was visualized by application of the

171 NovaRED™ substrate kit (Vector Laboratories). Sections were counterstained with Harris's
172 haematoxylin, dehydrated and mounted.

173

174 Hybridomas secreting monoclonal antibodies (mAbs) to porcine CD107a (4E9/11, IgG1), CD163
175 (2A10/11, IgG1), CD172a (BA1C11, IgG1) and BA4D5 (IgG2b) were derived from fusion of
176 myeloma cells with spleen cells from Balb/c mice immunized with pulmonary alveolar
177 macrophages. The characterization of these mAbs has been described elsewhere (Bullido et al.,
178 1997; Sánchez et al., 1999; Álvarez et al., 2000; Ezquerro et al., 2009). MAb were used in the
179 assays as hybridoma supernatants.

180

181 Labelled cells were analysed in 25 non-overlapping and consecutive high magnification fields of
182 0.2 mm². The expression of all markers was manually counted and the results were expressed as the
183 number of cells per mm².

184

185 **3. Results**

186 *3.1. Thymus from PR11- and PR40-infected pigs at 10-14 dpi showed strong inflammatory response*
187 *of the stroma and extensive cell death phenomena in the cortex*

188 The clinical signs and gross lesions have been previously described elsewhere (Canelli et al., 2017,
189 2018). Mortality rate was similar in the two infected groups, with two and three pigs euthanized due
190 to welfare conditions in PR40 and PR11 groups, respectively, between 10 and 14 dpi. Lung lesions
191 were more severe in the PR40 group compared to the PR11 group and consisted of interstitial
192 pneumonia with multifocal, mottled, tanned appearance of the lungs accompanied, in some cases,
193 by bronchopneumonia associated to secondary bacterial infections. Atrophy of the thymus was
194 detected in both infected groups, with an almost complete atrophy of the cervical part of the thymus
195 in the PR40 group. Control animals did not exhibit significant gross or microscopic lesions.

196

197 The thymus of the infected animals groups with any of both viruses (either PR11 or PR40) was
198 characterised by diffuse cortical reduction, disappearance of the corticomedullary boundary, and, in
199 some cases, a consistent inflammation of the stroma. The most intense changes were observed in
200 the thymus from PR11- and PR40-infected pigs that died at 10-14 dpi, which presented extensive
201 cell death phenomena in the cortex with a strong disappearance of the corticomedullary boundary
202 (Table 2) (Fig. 2A-2B). In most of these animals, a marked interstitial inflammatory infiltrate of the
203 stroma by abundant neutrophils and mononuclear cells (macrophages, lymphocytes and plasma
204 cells in a lesser extent) together with oedema of the connective tissue was also observed (Fig. 2C).
205 This infiltrate was particularly intense at perivascular area and was associated with intravascular
206 trafficking of these immune cells (Fig. 2D).

207

208 *3.2. PRRSV N protein positive cells were increased in PR40- and PR11-infected animals at 10-14*
209 *dpi mainly associated to the inflammatory foci in the stroma*

210 PRRSV N protein was not detected in the thymus of control animals (groups C and VAC-C).
211 PRRSV antigen was observed in the cytoplasm of macrophages from the thymic cortex and the
212 stroma, and in a lesser extent in macrophages from the medulla of the thymus of PR40 and PR11
213 infected animals at 35 dpi (Fig. 3A). Interestingly, PR40 and PR11 infected animals that died
214 between 10-14 dpi, presented a marked increase in the number of PRRSV positive cells, mainly
215 associated to a marked infiltrate of PRRSV positive cells within the inflammatory reaction observed
216 in the stroma of these animals (Fig. 3B-3C).

217

218 In case of vaccinated PR40-inoculated animals (VAC-PR40), only 3 out of 5 animals presented
219 PRRSV positive cells with a similar frequency and distribution than non-vaccinated PR40-
220 inoculated animals at 35 dpi.

221

222 *3.3. TUNEL labelling was increased in association to an intense increase of cell death in the cortex*

223 TUNEL labelling was mainly observed within tingible body macrophages in phagocytised non-fully
224 degraded cellular fragments and occasionally in free apoptotic bodies (Fig. 3D). TUNEL staining
225 was mostly observed in the cortex and, to a lesser extent, in the medulla of the thymus of all piglets.
226 No differences were observed either between infected animals and controls or among infected
227 groups at 35 dpi (Table 2). However, a marked increase of TUNEL labelling was observed in the
228 cortex of PR11 and PR40 infected animals at 10-14 dpi which showed a diffuse labelling associated
229 to an intense increase of cell death which occupied most of the cortex (Fig. 3E).

230

231 *3.4. CD172a positive cells were increased in the thymic cortex and stroma of PR11- and PR40-* 232 *infected pigs at 10-14 dpi*

233 Labelling against CD172a was mainly observed in the cell surface and cytoplasm of monocytes and
234 macrophages as well as, in a lesser extent, in granulocytes and occasionally in dendritic-like cells
235 (Fig. 4D). Tingible body macrophages did not stain for this marker. CD172a positive cells were
236 more numerous in the thymic medulla than in the cortex and stroma of control animals. The thymus
237 of the animals infected with PR11 and PR40 and killed at 35 dpi showed a similar distribution of
238 CD172a positive cells than the control group (Fig. 4A). Interestingly, the expression of CD172a in
239 PR11- and PR40-infected pigs that died at 10-14 dpi was dramatically different; specifically, these
240 animals presented a major increase of positive cells in the stroma and minor in the cortex, together
241 with a decrease of CD172a positive cells in the medulla (Fig. 4A). These changes were more
242 pronounced in PR40 infected animals which presented a stunning increase in the number of
243 CD172a positive cells in the stroma (Fig. 4A-4D). In addition, a marked increase in the number of
244 intravascular CD172a positive cells was observed within blood vessels of the cortex, medulla and
245 stroma from both PR11 and PR40 infected animals dead at 10-14 dpi and from PR40 infected
246 animals killed at 35 dpi (data not shown).

247

248 Both vaccinated groups (VAC-C and VAC-PR40) showed a similar distribution of CD172a positive
249 cells than control animals (CON), with a mild increase in the cortex and medulla of VAC-PR40
250 animals (Fig. 4A).

251

252 *3.5. A general increase of CD163 positive cells in cortex, medulla and stroma as well as at*
253 *intravascular level was observed in the PR40 group (10-14 dpi)*

254 CD163 positive immunolabelling was visualized in the cytoplasm and cell surface of positive
255 macrophages. Tingible body macrophages from the cortex were also stained ~~against~~with CD163
256 antibody (Fig. 4F). The highest number of cells expressing CD163 was found in the thymic cortex
257 for all groups. In the control group, the expression of CD163 was also detected in the medulla and,
258 secondly, in the stroma. A general increase in the number of CD163 positive cells was observed in
259 the cortex and in the stroma of infected animals; particularly, in PR40-infected pigs that died at 10-
260 14 dpi, which showed an overall enhancement in the three compartments (cortex, medulla and
261 stroma) together with a moderate increase in the frequency of intravascular CD163 positive cells in
262 the cortex and the medulla (Fig. 4B-4F).

263

264 No changes were observed in the distribution of CD163 positive cells in the thymus of VAC-C and
265 VAC-PR40 animals (Fig. 4B).

266

267 *3.6. The number of CD107a positive cells was decreased in all infected animals*

268 The staining for CD107a was mainly observed in the cytoplasm of macrophages, being also
269 observed in tingible body macrophages from the cortex (Fig. 5C). The number of CD107a positive
270 cells in all experimental groups, except for the control group (CON), was lower than the one
271 detected for CD172a and CD163 positive cells (Fig. 5A). In control animals, the expression of
272 CD107a was mainly found in the thymic cortex, with lower expression in the medulla and only few
273 positive cells in the stroma. A general decrease in the number of CD107a positive cells was

274 observed in all infected animals with only a moderate increase being observed in the stroma of
275 PR11- and PR40-infected animals at 10-14 dpi (Fig. 5A-5D).

276

277 Interestingly, vaccinated groups (VAC-C and VAC-PR40) presented a similar trend among them
278 showing the lowest number of CD107a positive cells (Fig. 5A).

279

280 *3.7. A mild increase of BA4D5 positive cells was observed in PR11- and PR40-infected pigs at 10-*
281 *14 dpi and in vaccinated groups*

282 The staining for BA4D5 was very low in all experimental groups being observed in the cytoplasm
283 of macrophages of cortex, medulla and stroma of the thymus (Fig. 5B). Perivascular positive cells
284 were found in the thymic medulla of some animals, whereas intravascular positive cells were
285 scattered (Fig. 5E-5F). No changes were observed in PR11- and PR40-infected animals at 35 dpi
286 when compared with control animals. The animals infected with PR11 and PR40 that died at 10-14
287 dpi showed an increase of BA4D5 positive cells in the cortex and in a lesser extent in the stroma
288 (Fig. 5B). Vaccinated groups displayed an increase in the number of positive cells to this marker in
289 the medulla and in the stroma, being more pronounced in the VAC-C group (Fig. 5B).

290

291 **4. Discussion**

292 Porcine Reproductive and Respiratory Syndrome (PRRS) is one of the main viral diseases in pig
293 production, causing huge economic losses to the industry. A high genetic variability has been
294 reported for PRRSV, leading to the current recognition of two independent viral species (PRRSV1
295 and PRRSV2) (Adams et al., 2017) with also a marked intraspecies variability (Stadejek et al.,
296 2008; Stadejek et al., 2013). During the last decade, several PRRS outbreaks characterised by
297 severe clinical signs as well as high morbidity and mortality rates have been reported in many
298 countries from Europe and Southeast Asia (Lunney et al., 2010). Thus, Canelli and co-authors
299 (2017) characterised the strain PR40/2014, an Italian variant of the so-called HP-PRRSV1 subtype

300 1. According to the severe clinical signs and lesions observed in HP-PRRSV outbreaks as well as
301 the partial cross-protection conferred by commercial MLV vaccines, the study of the host-pathogen
302 interaction, with special emphasis on the role of target and primary lymphoid organs, such as the
303 thymus, is imperative. Therefore, the present study describes the impact of the infection with
304 PRRSV1 strains of different virulence, namely PR11/2014 and PR40/2014, on the macrophages
305 population of the thymus. Furthermore, the effect of a heterologous vaccination in the thymus of
306 animals challenged with the virulent strain PR40 was examined.

307

308 Thymic atrophy was observed in both PR11- and PR40-infected animals with more intense changes
309 in animals that died at 10-14 dpi. Microscopically, no differences were observed among both
310 infected groups, which presented disappearance of the corticomedullary boundary, extensive cell
311 death phenomena in the cortex and a stunning oedema and interstitial infiltration of the stroma at
312 10-14 dpi. However, the highest number of PRRSV positive cells was observed in a PR40-infected
313 animal dead at 10 dpi. Our results agree with previous reports that describe a trend for highly
314 pathogenic strains of the virus to highly replicate in the thymus (Butler et al., 2014), but contrast
315 with the thymus atrophy, cortical T cell depletion and consequent dysfunction of host immune
316 regulation associated to the virulence of the PRRSV strain (Amarilla et al., 2016; Han et al., 2017).
317 These discrepancies may be associated to the intrinsic differences between each experimental
318 setting as well as to the criteria for classifying a PRRSV strain as a virulent strain. Thus, exhaustive
319 criteria need to be established to categorize the virulence of PRRSV strains.

320

321 PRRSV is well known by its ability to induce cell death, being TUNEL labelling widely used for
322 the assessment of this goal (He et al., 2012; Gómez-Laguna et al., 2013; Amarilla et al., 2016). In
323 the present study, TUNEL ~~stainingstainingpositive cells were was~~ mainly found in cellular
324 fragments phagocytised by tingible body macrophages and apoptotic bodies from the thymic cortex
325 at 35 dpi. Noteworthy, pigs infected with PR11 and PR40 strains that died at 10-14 dpi presented

326 marked cell death phenomena in the cortex (Grade IV) with an intense and diffuse TUNEL
327 labelling. These animals also showed a higher number of PRRSV positive cells compared with
328 infected animals at 35 dpi. The severity of cell death phenomena in these animals together with the
329 number and location of PRRSV positive cells support the role of both direct and indirect induction
330 of cell death by PRRSV (Rodríguez-Gómez et al., 2013).

331

332 The remarkable inflammatory reaction observed in the stroma of the thymus at 10-14 dpi was
333 associated with a high number of PRRSV positive cells both in the cortex and in the stroma of the
334 thymus. These findings suggest that during the acute phase of the disease, PRRSV may be able to
335 actively replicate and disseminate, reaching other organs besides lungs, such as the thymus, through
336 haematogenous dissemination. This hypothesis is also supported by the peak of viremia at 10 dpi
337 (PR11 group) and 7 dpi (PR40 group) detected in a parallel study by Canelli and co-authors (2017).

338

339 PR40-vaccinated animals (VAC-PR40) presented minimal histopathological lesions in the thymus
340 when compared with vaccinated control animals (VAC-C). In addition, a low number of PRRSV
341 positive cells was detected in the thymus of vaccinated and challenged animals. These results agree
342 with the partial protection conferred by MLV vaccines previously reported by other authors (Trus et
343 al., 2014; Do et al., 2015; Bonckaert et al., 2016; Canelli et al., 2018) and highlight the role of
344 heterologous vaccination in controlling the extension of the lesions and the spread of the virus in
345 animals infected with a virulent PRRSV strain.

346

347 Macrophages are a central myeloid component of the innate immune system. They are not only
348 activators but also one of the main regulators of the inflammation, being implicated in its resolution
349 and in triggering off the reparative process. Herein, the macrophage population of the thymus was
350 examined by CD172a, CD163, CD107a and BA4D5 immunolabelling. These markers have been
351 previously used in many studies to characterise porcine tissue macrophages (Bullido et al., 1997;

352 Domenech et al., 2003; Pérez et al., 2008). CD172a is one of the markers most commonly used and
353 identifies myeloid cells from precursor stages until cellular differentiation (Summerfield et al.,
354 1997). CD163, recognised as a major receptor for PRRSV ([Calvert et al., 2007](#))(~~[Van Breedam et al.,](#)~~
355 ~~[2010](#)~~), play also a role as a scavenger receptor and in the induction of the anti-inflammatory
356 mediators haptoglobin and IL-10 (Philippidis et al., 2004). Moreover, CD107a is directly related to
357 the cytotoxic activity and has been demonstrated to be a useful marker of macrophage populations
358 in tissues (Bullido et al., 1997; Aktas et al., 2008).

359

360 Our results showed no differences in CD172a immunolabelling between control group, infected
361 animals at 35 dpi and vaccinated animals. However, an enhancement in the number of CD172a
362 positive cells was observed in the cortex and especially in the stroma of infected animals at 10-14
363 dpi. These changes were more pronounced in PR40-infected pigs which also presented positive
364 cells within the blood vessels. The number of CD163 positive cells was increased in infected
365 animals throughout the study, and particularly in PR40-infected pigs at 10-14 dpi which displayed a
366 general increase of CD163 labelling in all the compartments (cortex, medulla and stroma) with
367 abundant intravascular CD163 positive cells. The increase in the number of CD172a and CD163
368 positive cells observed in both infected groups at 10-14 dpi was associated with the marked
369 inflammatory infiltrate of the stroma of the thymus as well as with the extensive cell death of
370 cortical thymocytes. Thus, monocytes/macrophages may be migrating from the bloodstream and
371 other tissues to the thymus through chemotaxis from inflammatory foci as well as from a high
372 demand of phagocytosis of cell death debris in the thymic cortex. The identification of intravascular
373 CD172a and CD163 positive cells observed in the present study supports this hypothesis.
374 Furthermore, the increase in the number of CD163 positive cells may also get along with the
375 induction of this surface molecule in resident tissue macrophages from the thymus. Interestingly,
376 the induction of CD163 has been proved in CD163 negative monocytes from bone marrow after *in*
377 *vitro* PRRSV infection (Fernández-Caballero et al.,2018) The higher frequency of CD163 positive

378 cells observed in both infected groups along our study may answer to different strategies of the
379 virus: (1) to increase the number of susceptible cells to virus replication (Patton et al. 2009); (2) to
380 allow PRRSV persistence in the thymus (Patton et al. 2009); (3) to lead to the modulation of the
381 inflammatory and immune response through the induction of haptoglobin and IL-10 (Philippidis et
382 al., 2004) or (4) to increase the phagocytic activity of macrophages through the binding of the
383 scavenger receptor to Gram-positive and Gram-negative bacteria (Fabriek et al., 2009).

384

385 CD107a immunolabelling was mainly found in the thymic cortex in the control group, while a
386 generalised decrease in the frequency of positive cells was observed in infected animals, with the
387 only exception of infected animals at 10-14 dpi, which presented a mild increase of CD107a
388 positive cells in the stroma. Compared with the other markers, the number of BA4D5 positive cells
389 was much lower, with an enhancement in the number of positive cells mainly in the cortex of both
390 infected groups at 10-14 dpi and in a lesser extent in the thymic medulla of vaccinated animals. The
391 decrease in the number of CD107a positive cells together with the increase in the number of
392 BA4D5 positive cells highlight different mechanisms of regulation of the cytotoxic activity not only
393 in infected pigs but also in vaccinated animals, which may be potentially involved in the
394 modulation of the host immune response. BA4D5 antibody is thought to be specific for porcine
395 CD68, which is mainly expressed by cells from the monocyte lineage, by circulating macrophages
396 and by tissue macrophages (Taylor et al., 2005). Among other functions CD68 plays a role in the
397 cytotoxic activity, with a predominant intracellular location in phagolysosomes (Kurushima et al.,
398 2000); phagocytic activity, associated to the scavenger receptor family and promoting cellular
399 debris clearance (Taylor et al., 2005) and mediating the recruitment and activation of macrophages
400 through binding to specific lectins and selectins (Song et al., 2011). In our study, the increase in the
401 number of perivascular and intravascular BA4D5 positive cells observed in animals from both
402 infected groups at 10-14 dpi as well as in vaccinated animals support the potential role of this
403 molecule in macrophages recruitment observed mainly in infected pigs at 10-14 dpi.

404

405 The main evidence observed in the present work was the presence of severe histopathological
406 lesions in the thymus of the animals infected with PR11 and PR40 PRRSV strains that died at 10-14
407 dpi, and the increase in the number of macrophages in the different compartments of the thymus.
408 The different markers used in this study allow us identifying the recruitment of macrophages
409 associated to the strong and early inflammatory response in the stroma of the thymus, the increase
410 in the expression of the major receptor of PRRSV and the regulation of the host cytotoxic activity
411 by macrophages. Interestingly, no marked differences were observed between the low virulent
412 PR11 and the virulent PR40 strains used in this study. Our results give some light to the
413 dysregulation of the host immune response by PRRSV and how the infection of the macrophage
414 population during the early phases of the disease may influence the decrease of the T cell
415 population, already demonstrated in other studies (Canelli et al., 2017). Finally, our results point out
416 that heterologous vaccination is a useful strategy to restrain virus spread as well as the extent of the
417 lesions observed in animals infected with virulent strains of PRRSV.

418

419 **Acknowledgements**

420 The authors would like to thank Gema Muñoz and Alberto Alcántara for their technical assistance.
421 Giulia Ogno is funded by a pre-doctoral grant of the Department of Veterinary Science, University
422 of Parma, Italy. Dr. Elena Canelli was funded by grants of the Department of Veterinary Science,
423 University of Parma. J. Gómez-Laguna is supported by a “Ramón y Cajal” contract of the Spanish
424 Ministry of Economy and Competitiveness (RYC-2014-16735). This work was partially supported
425 by the Spanish Ministry of Education and Science (Grant #AGL2016-76111-R).

426

427 **References**

428 Adams, M.J., Lefkowitz, E.J., King, A.M.Q., Harrach, B., Harrison, R.L., Knowles, N.J., Kropi
429 nski, A.M., Krupovic, M., Kuhn, J.H., Mushegian, A.R., Nibert, M., Sabanadzovic, S., Sa

430 nfaçon, H., Siddell, S.G., Simmonds, P., Varsani, A., Zerbini, F.M., Gorbalenya, A.E., D
431 avison, A.J., 2017. Changes to taxonomy and the international code of virus
432 classification and nomenclature ratified by the International Committee on Taxonomy of
433 Viruses. *Arch Virol.* 162, 2505–2538. doi:10.1007/s00705-017-3358-5.

434 Amarilla, S.P., Gómez-Laguna, J., Carrasco, L., Rodríguez-Gómez, I.M., Caridad, Y.O.J.M.,
435 Graham, S.P., Frossard, J.P., Steinbach, F., Salguero, F.J., 2016. Thymic depletion of
436 lymphocytes is associated with the virulence of PRRSV-1 strains. *Vet. Microbiol.* 188,
437 47-58. <https://doi.10.1016/j.vetmic.2016.04.005>.

438 Álvarez, B., Sánchez, C., Bullido, R., Marina, A., Lunney, J., Alonso, F., Ezquerro, A.,
439 Domínguez, J., 2000. A porcine cell surface receptor identified by monoclonal
440 antibodies to SWC3 is a member of the signal regulatory protein family and associates
441 with protein- tyrosine phosphatase SHP-1. *Tissue Antigens* 55, 342–351.

442 Aktas, E., Kucuksezer, U.C., Bilgic, S., Erten, G., Deniz, G., 2008. Relationship between
443 CD107a expression and cytotoxic activity. *Cell Immunol.* 254, 149–154. doi:
444 10.1016/j.cel- limm.2008.08.007 PMID:18835598. ☒

445 Balka, G., Podgórska, K., Brar, M.S., Bálint, Á., Cadar, D., Celer, V., Dénes, L., Dirbakova, Z.,
446 Jedryczko, A., Márton, L., Novosel, D., Petrović, T., Sirakov, I., Szalay, D., Toplak, I.,
447 Leung, F.C., Stadejek, T., 2018. Genetic diversity of PRRSV 1 in Central Eastern
448 Europe in 1994-2014: origin and evolution of the virus in the region. *Sci Rep.* 8, 7811.
449 doi: 10.1038/s41598-018-26036-w.

450 Barranco, I., Gómez-Laguna, J., Rodríguez-Gómez, I.M., Quereda, J.J., Salguero, F.J., Pallarés,
451 F.J., Carrasco, L., 2012. Immunohistochemical expression of IL-12, IL-10, IFN-alpha
452 and IFN-gamma in lymphoid organs of porcine reproductive and respiratory syndrome
453 virus-infected pigs. *Vet. Immunol. Immunopathol.* 149, 262–271.
454 <https://doi.10.1016/j.vetimm.2012.07.011>.

455 Bonckaert, C., Van der Meulen, K., Rodriguez-Ballara, I., Sanz, P., Fenech Martinez, P.,
456 Nauwynck, H., 2016. Modified-live PRRSV subtype 1 vaccine UNISTRAIN PRRS
457 provides a partial clinical and virological protection upon challenge with East European
458 subtype 3 PRRSV strain Lena. P.H.M. 2, 12. doi: 10.1186/s40813-016-0029-y.

459 Bullido, R., Gomez del Moral, M., Alonso, F., Ezquerra, A., Zapata, A., Sánchez, C., et
460 al.,1997. Monoclonal antibodies specific for porcine monocytes/macrophages:
461 macrophage heterogeneity in the pig evidenced by the expression of surface antigens.
462 Tissue Antigens. 49, 403–13. <https://doi.org/10.1111/j.1399-0039.1997.tb02769.x>

463 [Burkard, C., Lillico, S.G., Reid, E., Jackson, B., Mileham, A.J., Ait-Ali, T., Whitelaw,](#)
464 [C.B.A., Archibald, A.L.,2017. Precision engineering for PRRSV resistance in pigs:](#)
465 [Macrophages from genome edited pigs lacking CD163 SRCR5 domain are fully resistant](#)
466 [to both PRRSV genotypes while maintaining biological function. Plos pathogens.](#)
467 [13\(2\):e1006206 https://doi.org/10.1371/journal.ppat.1006206.](#)

468 Butler, J.E., Lager, K.M., Golde, W., Faaberg, K.S., Sinkora, M., Loving, C., Zhang, Y.I., 2014.
469 Porcine reproductive and respiratory syndrome (PRRS): An immune dysregulatory
470 pandemic. Immunol. Res. 59, 81–108. <https://doi.10.1007/s12026-014-8549-5>.

471 [Calvert, J.G., Slade, D.E., Shields, S.L., Jolie, R., Mannan, R.M., Ankenbauer, R.G., Welch,](#)
472 [S.K., 2007. CD163 expression confers susceptibility to porcine reproductive and](#)
473 [respiratory syndrome viruses. J Virol. 81,7371–9.](#)

474 Canelli, E., Catella, A., Borghetti, P., Ferrari, L., Ogno, G., De Angelis, E., Corradi, A., Passeri,
475 B., Bertani, V., Sandri, G., Bonilauri, P., Leung, F.C., Guazzetti, S., Martelli, P., 2017.
476 Phenotypic characterization of a highly pathogenic Italian porcine reproductive and
477 respiratory syndrome virus (PRRSV) type 1 subtype 1 isolate in experimentally infected
478 pigs. Vet Microbiol. 210, 124-133. <http://dx.doi.org/10.1016/j.vetmic.2017.09.002>.

479 Canelli, E., Catella, A., Borghetti, P., Ferrari, L., Ogno, G., Corradi, A., De Angelis, E.,
480 Bonilauri, P., Guazzetti, S., Martelli, P., 2018. Evaluation of the efficacy of a

481 commercial modified live virus vaccine against a highly pathogenic Italian PRRSV-1 in
482 experimentally infected pigs. *Veterinary Microbiology*. 226, 89-96.
483 <https://doi.10.1016/j.vetmic.2018.10.001>.

484 Do, D.T., Park, C., Choi, K., Jeong, J., Nguyen, T.T., Nguyen, K.D., Chae, C., 2015.
485 Comparison of two genetically distant type 2 porcine reproductive and respiratory
486 syndrome virus (PRRSV) modified live vaccines against Vietnamese highly pathogenic
487 PRRSV. *Vet. Microbiol.* 179, 233-241. doi: 10.1016/j.vetmic.2015.06.013.

488 Domenech, N., Rodriguez-Carreno, M.P., Filgueira, P., Alvarez, B., Chamorro, S., Domínguez,
489 J., 2003. Identification of porcine macrophages with monoclonal antibodies in formalin-
490 fixed, paraffin-embedded tissues. *Vet Immunol Immunopathol.* 94, 77-81.
491 [https://doi.org/10.1016/s0165-2427\(03\)00084-9](https://doi.org/10.1016/s0165-2427(03)00084-9).

492 Duan, X., Nauwynck, H.J., Pensaert, M.B., 1997. Virus quantification and identification of
493 cellular targets in the lungs and lymphoid tissues of pigs at different time intervals after
494 inoculation with porcine reproductive and respiratory syndrome virus (PRRSV). *Vet*
495 *Microbiol.* 56, 9-19. [https://doi.org/10.1016/S0378-1135\(96\)01347-8](https://doi.org/10.1016/S0378-1135(96)01347-8).

496 Ezquerro, A., Revilla, C., Alvarez, B., Perez, C., Alonso, F., Dominguez, J., 2009. Porcine
497 myelomonocytic markers and cell populations. *Dev. Comp. Immunol.* 33, 284-298.
498 <https://doi.org/10.1016/j.dci.2008.06.002>.

499 Fabriek, B. O., van Bruggen, R., Deng, D. M., et al., 2009. The macrophage scavenger receptor
500 CD163 functions as an innate immune sensor for bacteria. *Blood.* 113, no. 4, pp. 887-
501 892. ☒

502 [Frydas, I.S., Trus, I., Kvisgaard, L.K., Bonckaert, C., Reddy, V.R., Li, Y., Larsen, L.E.,](#)
503 [Nauwynck, H.J., 2015. Different clinical, virological, serological and tissue tropism](#)
504 [outcomes of two new and one old Belgian type 1 subtype 1 porcine reproductive and](#)

505 [respiratory virus \(PRRSV\) isolates. Vet Res 46, 37. https://doi: 10.1186/s13567-015-](https://doi.org/10.1186/s13567-015-0166-3)
506 [0166-3](https://doi.org/10.1186/s13567-015-0166-3)

507 Geissmann, F., Gordon, S., Hume, D.A., Mowat, A.M., Randolph, G.J., 2010. Unravelling
508 mononuclear phagocyte heterogeneity. Nat Rev Immunol. 10, 453–460. doi:
509 10.1038/nri2784.

510 Gómez-Laguna, J., Salguero, F.J., Barranco, I., Pallarés, F.J., Rodríguez-Gómez, I.M., Bernabé,
511 A., Carrasco, L., 2010. Cytokine expression by macrophages in the lung of pigs infected
512 with the porcine reproductive and respiratory syndrome virus. J. Comp. Pathol. 142, 51–
513 60. <https://doi.org/10.1016/j.jcpa.2009.07.004>.

514 Gómez-Laguna, J., Salguero, F.J., Pallarés, F.J., Carrasco, L., 2013. Immunopathogenesis of
515 porcine reproductive and respiratory syndrome in the respiratory tract of pigs. Vet. J.
516 195, 148–155. <https://doi.org/10.1016/j.tvjl.2012.11.012>.

517 [Gorbalenya, A.E., Krupovic, M., Siddell, S., Varsani, A., Kuhn, J.H., 2018. Riboviria:](https://doi.org/10.1016/j.tvjl.2012.11.012)
518 [establishing a single taxon that comprises RNA viruses at the basal rank of virus](https://doi.org/10.1016/j.tvjl.2012.11.012)
519 [taxonomy. International Committee on Taxonomy of Viruses:](https://doi.org/10.1016/j.tvjl.2012.11.012)
520 https://talk.ictvonline.org/taxonomy/p/taxonomy-history?taxnode_id=20186087

521 Han, J., Zhou, L., Ge, X., Guo, X. & Yang, H., 2017. Pathogenesis and control of the
522 Chinese highly pathogenic porcine reproductive and respiratory syndrome
523 virus. Veterinary microbiology. 209, 30–47.
524 <https://doi.org/10.1016/j.vetmic.2017.02.020>.

525 He, Y., Wang, G., Liu, Y., Shi, W., Han, Z., Wu, J., Jiang, C., Wang, S., Hu, S., Wen, H., Dong,
526 J., Liu, H., Cai, X., 2012. Characterization of thymus atrophy in piglets infected with
527 highly pathogenic porcine reproductive and respiratory syndrome virus. Vet. Microbiol.
528 160, 455–462. <https://doi.org/10.1016/j.vetmic.2012.05.040>.

529 Karniychuk, U.U., M. Geldhof, M. Vanhee, J. Van Doorselaere, T.A., Saveleva, Nauwynck, H.
530 J., 2010. Pathogenesis and antigenic characterization of a new East European subtype 3

531 porcine reproductive and respiratory syndrome virus isolate. BMC Vet. Res. 6, 30.
532 <https://doi.org/10.1186/1746-6148-6-30>.

533 Kurushima, H., Ramprasad, M., Kondratenko, N., Foster, D.M., Quehenberger, O., Steinberg
534 D., 2000. Surface expression and rapid internalization of macrosialin (mouse CD68) on
535 elicited mouse peritoneal macrophages. J. Leukoc. Biol. 67, 104–108.
536 <https://doi.org/10.1002/jlb.67.1.104>.

537 Law, S.K.A., Micklem, K.J., Shaw, J.M., Zhang, X.P., Dong, Y., Willis, A.C., Mason, , D.Y.,
538 1993. A new macrophage differentiation antigen which is a member of the scavenger
539 receptor superfamily. Eur. J. Immunol. 23, 2320–5.
540 <https://doi.org/10.1002/eji.1830230940>.

541 Lunney, J.K., Benfield, D.A., Rowland, R.R., 2010. Porcine reproductive and respiratory
542 syndrome virus: an update on an emerging and re-emerging viral disease of swine. Virus
543 Res. 154, 1–6. <https://doi.org/10.1016/j.virusres.2010.10.009>.

544 [Morgan, S.B., Graham, S.P., Salguero, F.J., Sánchez-Cordón, P.J., Mokhtar, H., Rebel, J.M.J.,](#)
545 [Weesendorp, E., Bodman-Smith, K.B., Steinbach, F., Frossard, J.P., 2013. Increased](#)
546 [pathogenicity of European porcine reproductive and respiratory syndrome virus is](#)
547 [associated with enhanced adaptive responses and viral clearance. Vet Microbiol 163, 13-](#)
548 [22. \[https://doi: 10.1016/j.vetmic.2012.11.024\]\(https://doi:10.1016/j.vetmic.2012.11.024\).](#)

549 Murtaugh, M.P., Stadejek, T., Abrahante, J.E., Lam, T.T., Leung, F.C., 2010. The ever-
550 expanding diversity of porcine reproductive and respiratory syndrome virus. Virus
551 Res. 154, 18-30. <https://doi.org/10.1016/j.virusres.2010.08.015>.

552 Nelsen, C. J., Murtaugh, M.P., Faaberg, K.S., 1999. Porcine reproductive and respiratory
553 syndrome virus comparison: divergent evolution on two continents. J Virol 73(1): 270-
554 280.

555 Patton, J.B., Rowland, R.R., Yoo, D., Chang, K.O., 2009. Modulation of CD163 receptor
556 expression and replication of porcine reproductive and respiratory syndrome virus in

557 porcine macrophages. *Virus Research*, vol. 140, no. 1-2, pp. 161–171, 2009.
558 <https://doi.org/10.1016/j.virusres.2008.12.002>.

559 Pearse, G., 2006a. Histopathology of the thymus. *Toxicol. Pathol.* 34, 515–547.

560 Pearse, G., 2006b. Normal structure, function and histology of the thymus. *Toxicol. Pathol.* 34,
561 504–514.

562 Perez, C., Ortuno, E., Gomez, N., Garcia-Briones, M., Alvarez, B., Martinez de la Riva, P.,
563 Alonso, F., Revilla, C., Domínguez, J., Ezquerro, A., 2008. Cloning and expression of
564 porcine CD163: its use for characterization of monoclonal antibodies to porcine CD163
565 and development of an ELISA to measure soluble CD163 in biological fluids. *Span J*
566 *Agric Res.* 6, 59–72. <https://doi.10.5424/sjar/200806S1-374>.

567 Philippidis, P., Mason, J.C., Evans, B.J., Nadra, I., Taylor, K.M., Haskard, D.O., Landlis, R.C.,
568 2004. Hemoglobin scavenger receptor CD163 mediates inter- leukin-10 release and
569 heme oxygenase-1 synthesis: anti-inflammatory monocyte-macrophage responses in
570 vitro, in resolving skin blisters in vivo, and after cardiopulmonary bypass surgery. *Circ*
571 *Res* 94, 119-126. <https://doi.10.1161/01.RES.0000109414.78907.F9>.

572 Rodríguez-Gómez, I.M., Gómez-Laguna, J., Carrasco, L., 2013. Impact of PRRSV on activation
573 and viability of antigen presenting cells. *World J. Virol.* 2, 146–151.
574 <https://doi.10.5501/wjv.v2.i4.146>.

575 [Sánchez, C., Domenech, N., Vázquez, J., Alonso, F., Ezquerro, A., Domínguez, J., 1999. The](#)
576 [porcine 2A10 antigen is homologous to human CD163 and related to macrophage](#)
577 [differentiation. *J Immunol.* 162, 5230–5237.](#)

578 [Sinn, L.J., Klingler, E., Lamp, B., Brunthaler, R., Weissenböck, H., Rumenapf, T., Ladinig, A.,](#)
579 [2016. Emergence of a virulent porcine reproductive and respiratory syndrome virus](#)
580 [\(PRRSV\) 1 strain in Lower Austria. *Porcine Health Manag* 2,](#)
581 [28. \[https://doi: 10.1186/s40813-016-0044-z\]\(https://doi:10.1186/s40813-016-0044-z\)](#)

582 Song, L., Lee, C., & Schindler, C., 2011. Deletion of the murine scavenger receptor
583 CD68. *Journal of Lipid Research*, 52(8), 1542–1550. <https://doi.10.1194/jlr.m015412>.

584 Stadejek, T., Oleksiewicz, M.B., Scherbakov, A.V., Timina, A.M., Krabbe, J.S., Chabros, K.,
585 Potapchuk, D., 2008. Definition of subtypes in the European genotype of porcine
586 reproductive and respiratory syndrome virus: nucleocapsid characteristics and
587 geographical distribution in Europe. *Arch Virol* 153, 1479-1488.
588 <https://doi.10.1007/s00705-008-0146-2>.

589 Stadejek, T., Stankevicius, A., Murtaugh, M.P., Oleksiewicz, M.B., 2013. Molecular evolution
590 of PRRSV in Europe: current state of play. *Vet Microbiol* 165, 21-28.
591 <https://doi.10.1016/j.vetmic.2013.02.029>.

592 [Stadejek, T., Larsen, L.E., Podgórska, K., Botner, A., Botti, S., Dolka, I., Fabisiak, M.,](#)
593 [Heegaard, P.M.H., Hjulsager, C.K., Huc, T., Kvisgaard, L.K., Sapierzynski, R., Nielsen,](#)
594 [J., 2017. Pathogenicity of three genetically diverse strains of PRRSV Type 1 in specific](#)
595 [pathogen free pigs. *Vet Microbiol* 209,13-19. \[https://doi: 10.1016/j.vetmic.2017.05.011\]\(https://doi:10.1016/j.vetmic.2017.05.011\).](#)

596 Summerfield, A., McCullough, K.C., 1997. Porcine bone marrow myeloid cells: phenotype and
597 adhesion molecule expression. *J Leukoc Biol.* 62, 176–85.
598 <https://doi.org/10.1002/jlb.62.2.176>.

599 Taylor, P.R., Martinez-Pomares, L., Stacey, M., Lin, H.H., Brown, G.D., Gordon, S., 2005.
600 *Annu Rev Immunol.* 23, 901-44.
601 <https://doi.10.1146/annurev.immunol.23.021704.115816>.

602 Tian, K., Yu, X., Zhao, T., Feng, Y., Cao, Z., Wang, C., Hu, Y., Chen, X., Hu, D., Tian, X., Liu,
603 D., Zhang, S., Deng, X., Ding, Y., Yang, L., Zhang, Y., Xiao, H., Qiao, M., Wang, B.,
604 Hou, L., Wang, X., Yang, X., Kang, L., Sun, M., Jin, P., Wang, S., Kitamura, Y., Yan,
605 J., Gao, G.F., 2007. Emergence of fatal PRRSV variants: unparalleled outbreaks of
606 atypical PRRS in China and molecular dissection of the unique hallmark. *PLoS One*

607 2:e526. <https://doi.10.1371/journal.pone.0000526>.

608 Trus, I., Bonckaert, C., van der Meulen, K., Nauwynck, H.J., 2014. Efficacy of an attenuated
609 European subtype 1 porcine reproductive and respiratory syndrome virus (PRRSV)
610 vaccine in pigs upon challenge with the East European subtype 3 PRRSV strain Lena.
611 *Vaccine* 32, 2995-3003. doi: 10.1016/j.vaccine.2014.03.077.

612 Van Breedam, W., Delputte, P. L., Van Gorp, H., Misinzo, G., Vanderheijden, N., Duan, X.,
613 Nauwynck, H.J., 2010. Porcine reproductive and respiratory syndrome virus entry into
614 the porcine macrophage. *Journal of General Virology* 91(7): 1659-1667.
615 <https://doi.10.1099/vir.0.020503-0>.

616 [Whitworth KM, Rowland, R.R., Ewen, C.L., Tribble, B.R., Kerrigan, M.A., Cino-Ozuna, A.G.,](#)
617 [Samuel, M.S., Lightner, J.E., McLaren, D.G., Mileham, A.J., Wells, K.D., Prather, R.S.,](#)
618 [2016. Gene-edited pigs are protected from porcine reproductive and respiratory](#)
619 [syndrome virus. *Nature Biotechnology*. 34: 20–22. doi: 10.1038/nbt.3434.](#)

620 **Figure captions**

621 **Fig. 1.** Experimental design

622 **Fig. 2.** Representative photomicrographs of the thymus from a control pig (A; Haematoxylin-eosin,
623 HE; Bar, 100 μm), a PR11-infected pig dead at 10-14 dpi with a strong disappearance of the
624 corticomedullary boundary (B; HE; Bar, 100 μm ; Hassall's corpuscles are identified with two black
625 arrows), and a PR40-infected pig dead at 10-14 dpi with a marked interstitial inflammatory infiltrate
626 of the stroma by abundant neutrophils and mononuclear cells (macrophages, lymphocytes and
627 plasma cells in a lesser extent) particularly intense at perivascular level is showed (C; HE; Bar,
628 100 μm ; a Hassall's corpuscle is identified with an asterisk). A higher magnification of the
629 perivascular infiltrate, highlighted with a black dashed line in C, is showed (D; HE; Bar, 50 μm).

630 **Fig. 3.** (A) Counts for PRRSV N protein positive cells in the thymic cortex (blue column), medulla
631 (red column), stroma (green column) and total (the empty circles represent individual values; the
632 mean is showed as a black solid line). (B) N protein positive cells (arrows) in the thymic cortex of a
633 PR11-infected pig that died at 10-14 dpi (IHC, Bar, 50 μm). (C) High number of N protein positive
634 cells in the stroma and in the thymic cortex of a PR40-infected pig that died at 10-14 dpi (IHC, Bar,
635 50 μm). *Inset*, detail of the cytoplasmic staining against PRRSV N protein in a macrophage from the
636 stroma of a PR40-infected pig that died at 10-14 dpi (IHC, Bar, 20 μm). (D) TUNEL labelling of
637 tingible body macrophages in the cortex of the thymus of a control animal (TUNEL, Bar, 50 μm).
638 (E) Marked increase of TUNEL labelling in the cortex of a PR11-infected animal at 10-14 dpi, with
639 a diffuse labelling associated to an intense increase of cell death (TUNEL, Bar, 50 μm).

640 **Fig. 4.** Counts for CD172a (A) and CD163 (B) positive cells in the thymic cortex (blue column),
641 medulla (red column), stroma (green column) and total (the empty circles represent individual
642 values; the mean is showed as a black solid line). (C) CD172a positive cells in the thymic medulla
643 of a PR40-infected animal and killed at 35 dpi (IHC, Bar, ~~5100~~510 μm). (D) An increased number of
644 CD172a positive cells in the stroma and the cortex of the thymus from a PR11-infected animal that
645 died at 10-14 dpi (IHC, Bar, ~~5100~~510 μm). *Inset*, detail of the cytoplasmic staining against CD172a in

646 several macrophages from the stroma of a PR11-infected pig that died at 10-14 dpi (IHC, Bar,
647 20µm). (E) Scattered CD163 positive cells in the cortex and medulla of the thymus from a PR11-
648 infected animal that died at 10-14 dpi (IHC, Bar, 50µm). (F) Numerous macrophages and tingible
649 body macrophages within the thymic cortex and stroma of a PR40-infected pig at 10-14 dpi (IHC,
650 Bar, 50µm). *Inset*, detail of the cytoplasmic staining against CD163 in macrophages from the
651 stroma of a PR40-infected pig at 10-14 dpi (IHC, Bar, 20µm).

652 **Fig. 5.** Counts for CD107a (A) and BA4D5 (B) positive cells in the thymic cortex (blue column),
653 medulla (red column), stroma (green column) and total (the empty circles represent individual
654 values; the mean is showed as a black solid line). (C) Numerous tingible body macrophages
655 immunolabelled against CD107a in the thymic cortex of a control animal at 35 dpi (IHC, Bar,
656 ~~2100~~µm). *Inset*, detail of the cytoplasmic staining against CD107a in a macrophage with
657 cytoplasmic prolongations in the thymic cortex from the same animal (IHC, Bar, 20µm). (D)
658 Scattered CD107a positive cells in the cortex and medulla of the thymus from a PR40-infected
659 animal that died at 10-14 dpi (IHC, Bar, ~~2100~~µm). (E) BA4D5 positive cells in the medulla and at
660 perivascular level in the thymus from a VAC-PR40 animal at the end of the study (IHC, Bar,
661 ~~250~~µm). (F) Higher magnification of another field of the thymus from the same animal with a
662 marked perivascular infiltrate by BA4D5 positive cells (IHC, Bar, 20µm).

663

664

665 **Table 1.** Clones, sources and dilutions of the primary antibodies used for the immunohistochemical detection of macrophages markers.

Specificity (clone)	Type of antibody	Commercial origin	Fixative	Blocking solution	Dilution	Antigen retrieval
Anti-PRRSV (clone SDOW17)	mAb	Rural Technologies Inc., Brookings, SD, USA	Formalin	BSA 1%	1:500	Protease Type XIV ^a
TUNEL	N.A.	Roche Diagnostics, Indianapolis, USA	Formalin	N.A.	N.A.	Proteinase K ^b
Anti-CD172a (BA1C11)	mAb	In house, INIA	Formalin	BSA 1%	Neat	Citrate pH 3.2
Anti-CD163 (2A10/11)	mAb	In house, INIA	Formalin	BSA 1%	Neat	Citrate pH 3.2
Anti-CD107a (4E9/11)	mAb	In house, INIA	Formalin	BSA 1%	Neat	Citrate pH 3.2
Anti-BA4D5 (BA4D5)	mAb	In house, INIA	Formalin	BSA 1%	Neat	Citrate pH 3.2

666 N.A.: Not applicable; ^aProtease Type XIV (Sigma-Aldrich): 8 min at 37 °C in water bath; ^bProteinase K (Roche): 15 min at 37 °C in heat incubator.

667

Table 2. Histopathology grading of the thymus of piglets from each experimental group and average number of tingible body macrophages and TUNEL positive cells (expressed as the mean \pm SD).

	CON (35 dpi)	PR11 (35 dpi)	PR40 (35 dpi)	PR11 (10-14 dpi)	PR40 (10-14 dpi)	VAC-C	VAC-PR40
Grades							
0	2/3	-	1/3	-	-	-	3/5
I	-	-	-	-	-	-	1/5
II	1/3	1/1	2/3	-	-	2/2	1/5
III	-	-	-	-	-	-	-
IV	-	-	-	3/3	2/2	-	-
Tingible body macrophages	9.87 \pm 1.79	7	8.87 \pm 6.82	ND*	ND*	13.1 \pm 8.63	10.4 \pm 1.79
TUNEL positive cells	54.97 \pm 63.40	67.91	43.53 \pm 31.07	ND*	ND*	53.82 \pm 40.20	53.18 \pm 34.59

ND*: Not determined due to extensive cell death of thymocytes in the cortex.

1 **Highlights**

- 2 • The impact of PRRSV strains of different virulence on thymic macrophages was
3 examined
- 4 • Animals died 10-14 days after PR40 or PR11 infection showed the most severe
5 lesions
- 6 • The number of N-protein⁺, CD172a⁺, CD163⁺ and BA4D5⁺ cells increased at 10-
7 14dpi
- 8 • No marked differences were observed between the PR11 and PR40 strains in this
9 study
- 10 • Vaccination restrained virus spread and lesions in thymus of PR40-infected animals

1
2
3 1 **Impact of PRRSV strains of different *in vivo* virulence on the macrophage population of the**
4 **thymus**
5
6 2
7 3
8
9

10 4 Giulia Ognò^a, Irene M. Rodríguez-Gómez^b, Elena Canelli^a, Inés Ruedas-Torres^b, Belén Álvarez^c,
11
12 5 Javier Domínguez^c, Paolo Borghetti^a, Paolo Martelli^{a,1}, Jaime Gómez-Laguna^{b,1,*}
13
14 6
15
16 7
17

18 8 ^a Department of Veterinary Science, University of Parma, Strada del Taglio, Parma, 10 – 43126,
19
20 9 Italy.
21

22 10 ^b Department of Anatomy and Comparative Pathology, Faculty of Veterinary Medicine, University
23
24 11 of Cordoba, International Excellence Agrifood Campus ‘ceiA3’, Córdoba, Spain.
25

26 12 ^c Department of Biotechnology, National Institute for Agricultural and Food Research and
27
28 13 Technology (INIA), Madrid, Spain.
29
30 14
31
32

33 15 ¹Both authors contributed equally as last authors
34
35 16
36
37 17
38

39 18 ***Corresponding author at:** Department of Anatomy and Comparative Pathology, Faculty of
40
41 19 Veterinary Medicine, University of Córdoba, 14071, Córdoba, Spain.
42

43
44 20 Tel.: +34 957 218 162. Fax: +34 057 218 682. Email: v92golaj@uco.es (J. Gómez-Laguna)
45
46
47
48
49
50
51
52
53
54
55
56
57
58
59
60

61
62
63 **21 Abstract**
64

65 22 The emergence of “highly pathogenic” isolates of porcine reproductive and respiratory syndrome
66 23 virus (HP-PRRSV) has raised new concerns about PRRS control. Cells from the porcine monocyte-
67 24 macrophage lineage represent the target for this virus, which replicates mainly in the lung, and
68 25 especially in HP-PRRSV strains, also in lymphoid organs, such as the thymus. This study aimed at
69 26 evaluating the impact of two PRRSV strains of different virulence on thymic macrophages as well
70 27 as after heterologous vaccination. After experimental infection with PR11 and PR40 PRRSV1
71 28 subtype 1 strains (low and high virulent, respectively) samples from thymus were analysed by
72 29 histopathology and immunohistochemistry for PRRSV N protein, TUNEL, CD172a, CD163,
73 30 CD107a and BA4D5 expression. Mortality was similar in both infected groups, but lung lesions and
74 31 thymus atrophy were more intense in PR40 group. Animals died at 10-14 dpi after PR11 or PR40
75 32 infection showed the most severe histopathological lesions, with a strong inflammatory response of
76 33 the stroma and extensive cell death phenomena in the cortex. These animals presented an increase
77 34 in the number of N protein, CD172a, CD163 and BA4D5 positive cells in the stroma and the cortex
78 35 together with a decrease in the number of CD107a positive cells. Our results highlight the
79 36 recruitment of macrophages in the thymus, the increase in the expression of CD163 and the
80 37 regulation of the host cytotoxic activity by macrophages. However, no marked differences were
81 38 observed between PR11- and PR40-infected animals. Heterologous vaccination restrained virus
82 39 spread and lesions extent in the thymus of PR40-infected animals.
83
84
85
86
87
88
89
90
91
92
93
94
95
96
97
98
99
100
101
102

103 40
104
105
106 41 *Keywords:* virulence; PRRSV; macrophages; thymus; cell death.
107
108
109
110
111
112
113
114
115
116
117
118
119
120

1. Introduction

Porcine reproductive and respiratory syndrome virus (PRRSV) is a major swine pathogen that induces severe respiratory symptoms in growing and finishing pigs and reproductive failure in gilts and sows, causing considerable economic losses worldwide. The genome, of approximately 15 kb in length, consists of a positive-stranded RNA and contains 11 open reading frames (ORFs), coding for structural and non-structural proteins, which are subject to insertions and deletions determining the genetic diversity of the virus (Murtaugh et al., 2010). Recently, the two genotypes of the virus, type 1 or PRRSV1 (European) and type 2 or PRRSV2 (North American), have been included as different viral species within the genus *Betaarterivirus*, particularly *Betaarterivirus suid 1* species for PRRSV1 and *Betaarterivirus suid 2* species for the PRRSV2, respectively (Gorbalenya et al., 2018). Both viruses present high internal variability, with PRRSV1 being divided into at least four subtypes (pan-European subtype 1, encompassing different lineages, and East European subtypes 2, 3 and 4) and PRRSV2 into at least nine lineages (Nelsen et al., 1999; Stadejek, et al. 2006, 2013; Balka et al., 2018). During the last decade, virulent variants of the virus, referred to as highly pathogenic (HP), have emerged within both PRRSV1 and PRRSV2 (Lunney et al., 2010). These virulent strains often result in severe clinical signs, higher mortality rates and higher tropism and viral load in blood and tissues than low virulent PRRSV strains (Tian et al., 2007; Karnychuk et al., 2010; Canelli et al., 2017). Although virulent PRRSV1 strains have been traditionally associated to subtype 3 strains (Lena and SU1-bel strains), strains with similar characteristics have been identified within subtypes 1 (13V091, AUT15-33 and PR40/2014 strain) and 2 (BOR59 strain) (Karnychuk et al., 2010; Morgan et al., 2013; Frydas et al., 2015; Sinn et al., 2016; Canelli et al., 2017; Stadejek et al., 2017).

The efficacy of modified live virus (MLV) vaccines (PRRSV1 and PRRSV2) have been recently tested in challenge trials with virulent isolates (Trus et al., 2014; Do et al., 2015; Bonckaert et al., 2016; Canelli et al., 2018). Partial cross-protection of these vaccines against virulent strains has

181
182
183 68 been reported under experimental conditions with a reduction of the viremia, the severity of clinical
184
185 69 signs and lesions, and the duration of the clinical phase. Nevertheless, none of the tested vaccines
186
187 70 was able to prevent the transplacental transmission or the respiratory infection.
188
189
190 71

191
192 72 The main cell target for PRRSV replication is the pulmonary alveolar macrophage (PAM) but viral
193
194 73 replication has been also widely reported in other macrophage subpopulations from lungs as well as
195
196 74 from lymphoid organs of infected animals (Duan et al., 1997; Gómez-Laguna et al., 2010; Barranco
197
198 75 et al., 2012). Among lymphoid organs, the thymus particularly plays a central role in the
199
200 76 development of the immune system through the differentiation and maturation of T cells (Pearse et
201
202 77 al., 2006b). PRRSV infection is characterised by an immunosuppression state associated with,
203
204 78 among other factors, atrophy of the thymus and a major decrease in the number of thymocytes in
205
206 79 the cortex with marked differences according to the virulence of the PRRSV strain (Amarilla et al.,
207
208 80 2016). Thus, so-called HP-PRRSV strains cause more severe clinical signs, long-lasting viremia,
209
210 81 higher virus level in blood and tissues, and higher frequency of mortality (Lunney et al., 2010);
211
212 82 moreover, these strains predispose piglets to weak cellular immunity together with thymus atrophy,
213
214 83 T cell depletion and impairment of the development of naïve T cells (Han et al., 2017).
215
216 84

217
218
219 85 In a general context, macrophages perform three main functions: antigen presentation, phagocytosis
220
221 86 and synthesis and secretion of cytokines (Geissman et al., 2010). However, the whole range of
222
223 87 functions of thymic macrophages is still nowadays unclear. The macrophage population in the
224
225 88 thymus is evenly distributed in the cortex and in the medulla and is particularly designated, at least,
226
227 89 to phagocytose and remove apoptotic bodies and self-reactive lymphocytes as well as to release
228
229 90 mediators involved in thymocytes maturation (Pearse et al., 2006a). As a myeloid cell, the main
230
231 91 macrophage marker extensively used is CD172a, which is strongly expressed from the early stages
232
233 92 of differentiation onwards (Summerfield et al., 1997). A restricted marker to monocyte and
234
235 93 macrophages is CD163, a member of the family of proteins with scavenger receptor cysteine-rich
236
237
238
239
240

241
242
243 94 domains (Law et al., 1993). Particularly, CD163 has been identified to be the major receptor for
244
245 95 PRRSV uncoating and genome release (Calvert et al., 2007; Van Breedam et al., 2010), with well
246
247 96 described effects of the deletion of its SRCR5 domain on PRRSV infection (Whithworth et al.,
248
249
250 97 2016; Burkard et al., 2017). CD107a, or lysosomal-associated membrane protein 1 (LAMP-1),
251
252 98 despite not being restricted to macrophages, has been demonstrated to be useful for identifying
253
254 99 macrophages populations in tissue sections, especially, tingible body macrophages in lymphoid
255
256 100 organs as well as macrophages from the thymus cortex and medulla (Bullido et al., 1997;
257
258 101 Domenech et al., 2003). An interesting marker with a restricted expression for the macrophage
259
260 102 lineage is the antigen recognized by the monoclonal antibody BA4D5, which shows features that
261
262 103 resemble those of CD68. Thus, this molecule/antigen presents a predominant intracellular location
263
264 104 in phagolysosomes with a low expression on the cell surface and has been detected on macrophages
265
266
267 105 from the thymus cortex as well as on other macrophages from spleen and lymph nodes (Ezquerria et
268
269 106 al., 2009).

270
271 107
272
273 108 Considering the role of macrophages in PRRSV replication and on the onset of the host immune
274
275 109 response, the impact of two Italian subtype 1 PRRSV1 strains (PR40/2014 and PR11/2014), with
276
277 110 different *in vivo* virulence (Canelli et al., 2017), was evaluated in this study. In addition, the effect
278
279 111 of a heterologous vaccination on histopathological lesions as well as on macrophages populations of
280
281 112 the thymus of HP-PRRSV infected animals was examined.
282
283

284 113 285 286 114 **2. Materials and Methods**

287 288 115 *2.1. Animals and experimental infection*

289
290 116 The *in vivo* study is part of a large project carried out to investigate the pathogenesis and control of
291
292 117 PRRSV1 strains of differing virulence; materials analysed in the present study were collected from
293
294 118 experiments published elsewhere (Canelli et al., 2017, 2018). Briefly, a total of twelve 4-week-old
295
296 119 conventional pigs were assigned to three different experimental groups, as described in Canelli et
297
298
299
300

301
302
303 120 al. (2017): (i) PR40 group (PR40), with 5 pigs inoculated intra-nasally (IN) with 2 ml, containing
304
305 121 10^5 TCD₅₀ of PRRSV1 PR40/2014, per pig; (ii) PR11 group (PR11), with 4 piglets inoculated IN
306
307
308 122 with 2 ml, containing 10^5 TCD₅₀ of PRRSV1 PR11/2014, per pig; and, (iii) Control group (C), with
309
310 123 3 animals inoculated IN with sterile medium (mock/negative control). In addition, two different
311
312 124 vaccinated groups, described in Canelli et al. (2018), were included: (i) VAC-C: 2 pigs were IM-
313
314 125 vaccinated against PRRSV at 4 weeks of age (Porcilis® PRRS, MSD Animal Health; DV strain;
315
316 126 vaccine batch A208AD01) and left uninfected; (ii) VAC-PR40: 6 pigs were IM-vaccinated against
317
318 127 PRRSV and IN infected with PR40 at 35 days post-vaccination (dpv) (day 0 post-inoculation, dpi)
319
320 128 (Fig. 1).
321

322 129
323
324
325 130 No relevant pathogens (PRRSV, SIV, PCV2) were detected in the animals before the beginning of
326
327 131 the studies. Animals suffering from severe clinical signs with a fatal prognosis were humanely
328
329 132 euthanized according to standard protocols. All the survivors were humanely euthanized at 35 dpi
330
331 133 (end of the experiment). At necropsy gross pathology was recorded and thymus samples were
332
333 134 collected and fixed in buffered-formalin pH 7.4 for histopathology and immunohistochemical
334
335 135 studies. The experimental design and all the procedures were fully in agreement and approved by
336
337 136 the Ethical Committee and by the Ministry of Health in Italy according to European and National
338
339 137 rules on experimental infection studies and animal welfare.
340

341 138 342 343 139 *2.2. Histopathology and grading of thymus*

344
345 140 Four μm tissue sections were stained with haematoxylin and eosin (H&E). The severity of the
346
347
348 141 lesions in thymus was scored as follows (adapted and modified from Amarilla et al., 2016): (i)
349
350 142 Grade 0, the cortex:medulla ratio (C/M) is about 2:1 with typical histological characteristics of the
351
352 143 thymus; (ii) Grade I, diffuse cortical reduction with focal cortical disappearance, 5–9 tingible body
353
354 144 macrophages/ mm^2 within the thymic cortex, typical medulla and stroma; (iii) Grade II, focal or
355
356 145 multifocal decrease of C/M (<2:1), decrease of cortical layer with slight proportional increase of the
357

361
362
363 146 stroma and 10–15 tingible body macrophages/mm² within the thymic cortex; (iv) Grade III, focal to
364
365 147 multifocal blurring of normal corticomedullary demarcation, increase of the stroma, occasional
366
367
368 148 increase in the number of lymphocytes, mast and plasma cells and ≥ 16 tingible body
369
370 149 macrophages/mm², with a “starry sky” appearance of the tissue; and, (v) Grade IV, extensive cell
371
372 150 death of cortical thymocytes with complete disappearance of corticomedullary boundary
373
374 151 demarcation and increase of the stroma.

375
376 152
377
378 153 Manual quantification of tingible body macrophages in thymic cortex was assessed in 25 non-
379
380 154 overlapping, consecutively selected high magnification fields of 0.2 mm². Results were expressed
381
382
383 155 as number of cells per mm².

384
385 156

387 157 *2.3. Immunohistochemistry*

388
389 158 The Avidin–Biotin–Peroxidase complex technique (ABC Vector Elite, Vector laboratories, USA)
390
391 159 was used for the immunolabelling of PRRSV antigen and the different macrophages markers.
392
393 160 Terminal dUTP Nick End-Labeling (TUNEL) was carried out by using a commercial kit (In Situ
394
395 161 Cell Death Detection Kit, POD, Roche, Germany) following manufacturer’s instructions. Briefly, 4
396
397 162 μm tissue sections were dewaxed and rehydrated in a gradient of ethanol, followed by endogenous
398
399
400 163 peroxidase inhibition with 3 % H₂O₂ solution in methanol for 30 minutes (min). After treatment
401
402 164 with different antigen retrieval methods (Table 1), the slides were washed with PBS (pH 7.4) and
403
404 165 incubated for 30 min at room temperature with 100 μl of blocking solution in a humid chamber.
405
406 166 Primary antibodies were incubated overnight at 4 °C in a humid chamber (see dilutions in Table 1
407
408 167 for each antibody), while for the negative controls the primary antibody was replaced by either an
409
410 168 isotype control or by blocking solution. Biotinylated secondary antibody was incubated for 30 min
411
412 169 at room temperature. An avidin-biotin-peroxidase complex (Vector Laboratories) was applied for
413
414 170 1 hour at room temperature in the darkness. Labelling was visualized by application of the
415

416
417
418
419
420

421
422
423 171 NovaRED™ substrate kit (Vector Laboratories). Sections were counterstained with Harris's
424
425 172 haematoxylin, dehydrated and mounted.
426
427
428 173
429
430 174 Hybridomas secreting monoclonal antibodies (mAbs) to porcine CD107a (4E9/11, IgG1), CD163
431
432 175 (2A10/11, IgG1), CD172a (BA1C11, IgG1) and BA4D5 (IgG2b) were derived from fusion of
433
434 176 myeloma cells with spleen cells from Balb/c mice immunized with pulmonary alveolar
435
436 177 macrophages. The characterization of these mAbs has been described elsewhere (Bullido et al.,
437
438 178 1997; Sánchez et al., 1999; Álvarez et al., 2000; Ezquerro et al., 2009). MABs were used in the
439
440 179 assays as hybridoma supernatants.
441
442 180
443
444
445 181 Labelled cells were analysed in 25 non-overlapping and consecutive high magnification fields of
446
447 182 0.2 mm². The expression of all markers was manually counted and the results were expressed as the
448
449 183 number of cells per mm².
450

451 184

452

453 185 **3. Results**

454

455 186 *3.1. Thymus from PR11- and PR40-infected pigs at 10-14 dpi showed strong inflammatory response*
456
457 187 *of the stroma and extensive cell death phenomena in the cortex*
458

459

460 188 The clinical signs and gross lesions have been previously described elsewhere (Canelli et al., 2017,
461
462 189 2018). Mortality rate was similar in the two infected groups, with two and three pigs euthanized due
463
464 190 to welfare conditions in PR40 and PR11 groups, respectively, between 10 and 14 dpi. Lung lesions
465
466 191 were more severe in the PR40 group compared to the PR11 group and consisted of interstitial
467
468 192 pneumonia with multifocal, mottled, tanned appearance of the lungs accompanied, in some cases,
469
470 193 by bronchopneumonia associated to secondary bacterial infections. Atrophy of the thymus was
471
472 194 detected in both infected groups, with an almost complete atrophy of the cervical part of the thymus
473
474 195 in the PR40 group. Control animals did not exhibit significant gross or microscopic lesions.
475

476

477 196

478

479

480

481
482
483 197 The thymus of the infected animals with any of both viruses (either PR11 or PR40) was
484
485 198 characterised by diffuse cortical reduction, disappearance of the corticomedullary boundary, and, in
486
487
488 199 some cases, a consistent inflammation of the stroma. The most intense changes were observed in
489
490 200 the thymus from PR11- and PR40-infected pigs that died at 10-14 dpi, which presented extensive
491
492 201 cell death phenomena in the cortex with a strong disappearance of the corticomedullary boundary
493
494 202 (Table 2) (Fig. 2A-2B). In most of these animals, a marked interstitial inflammatory infiltrate of the
495
496 203 stroma by abundant neutrophils and mononuclear cells (macrophages, lymphocytes and plasma
497
498 204 cells in a lesser extent) together with oedema of the connective tissue was also observed (Fig. 2C).
499
500 205 This infiltrate was particularly intense at perivascular area and was associated with intravascular
501
502 206 trafficking of these immune cells (Fig. 2D).
503
504
505 207

506
507 208 *3.2. PRRSV N protein positive cells were increased in PR40- and PR11-infected animals at 10-14*
508
509 209 *dpi mainly associated to the inflammatory foci in the stroma*

510
511 210 PRRSV N protein was not detected in the thymus of control animals (groups C and VAC-C).
512
513 211 PRRSV antigen was observed in the cytoplasm of macrophages from the thymic cortex and the
514
515 212 stroma, and in a lesser extent in macrophages from the medulla of the thymus of PR40 and PR11
516
517 213 infected animals at 35 dpi (Fig. 3A). Interestingly, PR40 and PR11 infected animals that died
518
519 214 between 10-14 dpi, presented a marked increase in the number of PRRSV positive cells, mainly
520
521 215 associated to a marked infiltrate of PRRSV positive cells within the inflammatory reaction observed
522
523 216 in the stroma of these animals (Fig. 3B-3C).
524
525
526 217

527
528 218 In case of vaccinated PR40-inoculated animals (VAC-PR40), only 3 out of 5 animals presented
529
530 219 PRRSV positive cells with a similar frequency and distribution than non-vaccinated PR40-
531
532 220 inoculated animals at 35 dpi.
533
534 221

535
536 222 *3.3. TUNEL labelling was increased in association to an intense increase of cell death in the cortex*
537

541
542
543 223 TUNEL labelling was mainly observed within tingible body macrophages in phagocytised non-fully
544
545 224 degraded cellular fragments and occasionally in free apoptotic bodies (Fig. 3D). TUNEL staining
546
547
548 225 was mostly observed in the cortex and, to a lesser extent, in the medulla of the thymus of all piglets.
549
550 226 No differences were observed either between infected animals and controls or among infected
551
552 227 groups at 35 dpi (Table 2). However, a marked increase of TUNEL labelling was observed in the
553
554 228 cortex of PR11 and PR40 infected animals at 10-14 dpi which showed a diffuse labelling associated
555
556 229 to an intense increase of cell death which occupied most of the cortex (Fig. 3E).
557
558 230
559
560 231 *3.4. CD172a positive cells were increased in the thymic cortex and stroma of PR11- and PR40-*
561
562 232 *infected pigs at 10-14 dpi*
563
564 233 Labelling against CD172a was mainly observed in the cell surface and cytoplasm of monocytes and
565
566
567 234 macrophages as well as, in a lesser extent, in granulocytes and occasionally in dendritic-like cells
568
569 235 (Fig. 4D). Tingible body macrophages did not stain for this marker. CD172a positive cells were
570
571 236 more numerous in the thymic medulla than in the cortex and stroma of control animals. The thymus
572
573 237 of the animals infected with PR11 and PR40 and killed at 35 dpi showed a similar distribution of
574
575 238 CD172a positive cells than the control group (Fig. 4A). Interestingly, the expression of CD172a in
576
577 239 PR11- and PR40-infected pigs that died at 10-14 dpi was dramatically different; specifically, these
578
579 240 animals presented a major increase of positive cells in the stroma and minor in the cortex, together
580
581 241 with a decrease of CD172a positive cells in the medulla (Fig. 4A). These changes were more
582
583
584 242 pronounced in PR40 infected animals which presented a stunning increase in the number of
585
586 243 CD172a positive cells in the stroma (Fig. 4A-4D). In addition, a marked increase in the number of
587
588 244 intravascular CD172a positive cells was observed within blood vessels of the cortex, medulla and
589
590 245 stroma from both PR11 and PR40 infected animals dead at 10-14 dpi and from PR40 infected
591
592 246 animals killed at 35 dpi (data not shown).
593
594 247
595
596
597
598
599
600

601
602
603 248 Both vaccinated groups (VAC-C and VAC-PR40) showed a similar distribution of CD172a positive
604
605 249 cells than control animals (CON), with a mild increase in the cortex and medulla of VAC-PR40
606
607
608 250 animals (Fig. 4A).

609
610 251
611
612 252 *3.5. A general increase of CD163 positive cells in cortex, medulla and stroma as well as at*
613
614 253 *intravascular level was observed in the PR40 group (10-14 dpi)*

615
616 254 CD163 positive immunolabelling was visualized in the cytoplasm and cell surface of positive
617
618 255 macrophages. Tingible body macrophages from the cortex were also stained with CD163 antibody
619
620 256 (Fig. 4F). The highest number of cells expressing CD163 was found in the thymic cortex for all
621
622 257 groups. In the control group, the expression of CD163 was also detected in the medulla and,
623
624 258 secondly, in the stroma. A general increase in the number of CD163 positive cells was observed in
625
626 259 the cortex and in the stroma of infected animals; particularly, in PR40-infected pigs that died at 10-
627
628 260 14 dpi, which showed an overall enhancement in the three compartments (cortex, medulla and
629
630 261 stroma) together with a moderate increase in the frequency of intravascular CD163 positive cells in
631
632 262 the cortex and the medulla (Fig. 4B-4F).

633 263
634
635 264 No changes were observed in the distribution of CD163 positive cells in the thymus of VAC-C and
636
637 265 VAC-PR40 animals (Fig. 4B).

638
639 266
640
641
642 267
643
644 268 *3.6. The number of CD107a positive cells was decreased in all infected animals*

645
646 269 The staining for CD107a was mainly observed in the cytoplasm of macrophages, being also
647
648 270 observed in tingible body macrophages from the cortex (Fig. 5C). The number of CD107a positive
649
650 271 cells in all experimental groups, except for the control group (CON), was lower than the one
651
652 272 detected for CD172a and CD163 positive cells (Fig. 5A). In control animals, the expression of
653
654 273 CD107a was mainly found in the thymic cortex, with lower expression in the medulla and only few
655
656 274 positive cells in the stroma. A general decrease in the number of CD107a positive cells was
657

661
662
663 274 observed in all infected animals with only a moderate increase being observed in the stroma of
664
665 275 PR11- and PR40-infected animals at 10-14 dpi (Fig. 5A-5D).
666
667
668 276
669
670 277 Interestingly, vaccinated groups (VAC-C and VAC-PR40) presented a similar trend among them
671
672 278 showing the lowest number of CD107a positive cells (Fig. 5A).
673

674 279
675
676 280 *3.7. A mild increase of BA4D5 positive cells was observed in PR11- and PR40-infected pigs at 10-*
677
678 281 *14 dpi and in vaccinated groups*
679
680 282 The staining for BA4D5 was very low in all experimental groups being observed in the cytoplasm
681
682 283 of macrophages of cortex, medulla and stroma of the thymus (Fig. 5B). Perivascular positive cells
683
684 284 were found in the thymic medulla of some animals, whereas intravascular positive cells were
685
686
687 285 scattered (Fig. 5E-5F). No changes were observed in PR11- and PR40-infected animals at 35 dpi
688
689 286 when compared with control animals. The animals infected with PR11 and PR40 that died at 10-14
690
691 287 dpi showed an increase of BA4D5 positive cells in the cortex and in a lesser extent in the stroma
692
693 288 (Fig. 5B). Vaccinated groups displayed an increase in the number of positive cells to this marker in
694
695 289 the medulla and in the stroma, being more pronounced in the VAC-C group (Fig. 5B).
696

697 290 698 699 291 **4. Discussion**

700
701 292 Porcine Reproductive and Respiratory Syndrome (PRRS) is one of the main viral diseases in pig
702
703 293 production, causing huge economic losses to the industry. A high genetic variability has been
704
705
706 294 reported for PRRSV, leading to the current recognition of two independent viral species (PRRSV1
707
708 295 and PRRSV2) (Adams et al., 2017) with also a marked intraspecies variability (Stadejek et al.,
709
710 296 2008; Stadejek et al., 2013). During the last decade, several PRRS outbreaks characterised by
711
712 297 severe clinical signs as well as high morbidity and mortality rates have been reported in many
713
714 298 countries from Europe and Southeast Asia (Lunney et al., 2010). Thus, Canelli and co-authors
715
716 299 (2017) characterised the strain PR40/2014, an Italian variant of the so-called HP-PRRSV1 subtype
717

721
722
723 300 1. According to the severe clinical signs and lesions observed in HP-PRRSV outbreaks as well as
724
725 301 the partial cross-protection conferred by commercial MLV vaccines, the study of the host-pathogen
726
727
728 302 interaction, with special emphasis on the role of target and primary lymphoid organs, such as the
729
730 303 thymus, is imperative. Therefore, the present study describes the impact of the infection with
731
732 304 PRRSV1 strains of different virulence, namely PR11/2014 and PR40/2014, on the macrophages
733
734 305 population of the thymus. Furthermore, the effect of a heterologous vaccination in the thymus of
735
736 306 animals challenged with the virulent strain PR40 was examined.
737
738 307
739
740 308 Thymic atrophy was observed in both PR11- and PR40-infected animals with more intense changes
741
742 309 in animals that died at 10-14 dpi. Microscopically, no differences were observed among both
743
744
745 310 infected groups, which presented disappearance of the corticomedullary boundary, extensive cell
746
747 311 death phenomena in the cortex and a stunning oedema and interstitial infiltration of the stroma at
748
749 312 10-14 dpi. However, the highest number of PRRSV positive cells was observed in a PR40-infected
750
751 313 animal dead at 10 dpi. Our results agree with previous reports that describe a trend for highly
752
753 314 pathogenic strains of the virus to highly replicate in the thymus (Butler et al., 2014), but contrast
754
755 315 with the thymus atrophy, cortical T cell depletion and consequent dysfunction of host immune
756
757 316 regulation associated to the virulence of the PRRSV strain (Amarilla et al., 2016; Han et al., 2017).
758
759 317 These discrepancies may be associated to the intrinsic differences between each experimental
760
761
762 318 setting as well as to the criteria for classifying a PRRSV strain as a virulent strain. Thus, exhaustive
763
764 319 criteria need to be established to categorize the virulence of PRRSV strains.
765
766 320
767
768 321 PRRSV is well known by its ability to induce cell death, being TUNEL labelling widely used for
769
770 322 the assessment of this goal (He et al., 2012; Gómez-Laguna et al., 2013; Amarilla et al., 2016). In
771
772 323 the present study, TUNEL staining was mainly found in cellular fragments phagocytised by tingible
773
774 324 body macrophages and apoptotic bodies from the thymic cortex at 35 dpi. Noteworthy, pigs
775
776 325 infected with PR11 and PR40 strains that died at 10-14 dpi presented marked cell death phenomena
777

781
782
783 326 in the cortex (Grade IV) with an intense and diffuse TUNEL labelling. These animals also showed a
784
785 327 higher number of PRRSV positive cells compared with infected animals at 35 dpi. The severity of
786
787
788 328 cell death phenomena in these animals together with the number and location of PRRSV positive
789
790 329 cells support the role of both direct and indirect induction of cell death by PRRSV (Rodríguez-
791
792 330 Gómez et al., 2013).
793
794 331
795
796 332 The remarkable inflammatory reaction observed in the stroma of the thymus at 10-14 dpi was
797
798 333 associated with a high number of PRRSV positive cells both in the cortex and in the stroma of the
799
800 334 thymus. These findings suggest that during the acute phase of the disease, PRRSV may be able to
801
802 335 actively replicate and disseminate, reaching other organs besides lungs, such as the thymus, through
803
804 336 haematogenous dissemination. This hypothesis is also supported by the peak of viremia at 10 dpi
805
806
807 337 (PR11 group) and 7 dpi (PR40 group) detected in a parallel study by Canelli and co-authors (2017).
808
809 338
810
811 339 PR40-vaccinated animals (VAC-PR40) presented minimal histopathological lesions in the thymus
812
813 340 when compared with vaccinated control animals (VAC-C). In addition, a low number of PRRSV
814
815 341 positive cells was detected in the thymus of vaccinated and challenged animals. These results agree
816
817 342 with the partial protection conferred by MLV vaccines previously reported by other authors (Trus et
818
819 343 al., 2014; Do et al., 2015; Bonckaert et al., 2016; Canelli et al., 2018) and highlight the role of
820
821 344 heterologous vaccination in controlling the extension of the lesions and the spread of the virus in
822
823 345 animals infected with a virulent PRRSV strain.
824
825
826 346
827
828 347 Macrophages are a central myeloid component of the innate immune system. They are not only
829
830 348 activators but also one of the main regulators of the inflammation, being implicated in its resolution
831
832 349 and in triggering off the reparative process. Herein, the macrophage population of the thymus was
833
834 350 examined by CD172a, CD163, CD107a and BA4D5 immunolabelling. These markers have been
835
836 351 previously used in many studies to characterise porcine tissue macrophages (Bullido et al., 1997;
837

841
842
843 352 Domenech et al., 2003; Pérez et al., 2008). CD172a is one of the markers most commonly used and
844
845 353 identifies myeloid cells from precursor stages until cellular differentiation (Summerfield et al.,
846
847 354 1997). CD163, recognised as a major receptor for PRRSV (Calvert et al., 2007), play also a role as
848
849
850 355 a scavenger receptor and in the induction of the anti-inflammatory mediators haptoglobin and IL-10
851
852 356 (Philippidis et al., 2004). Moreover, CD107a is directly related to the cytotoxic activity and has
853
854 357 been demonstrated to be a useful marker of macrophage populations in tissues (Bullido et al., 1997;
855
856 358 Aktas et al., 2008).
857
858 359
859
860 360 Our results showed no differences in CD172a immunolabelling between control group, infected
861
862 361 animals at 35 dpi and vaccinated animals. However, an enhancement in the number of CD172a
863
864 362 positive cells was observed in the cortex and especially in the stroma of infected animals at 10-14
865
866
867 363 dpi. These changes were more pronounced in PR40-infected pigs which also presented positive
868
869 364 cells within the blood vessels. The number of CD163 positive cells was increased in infected
870
871 365 animals throughout the study, and particularly in PR40-infected pigs at 10-14 dpi which displayed a
872
873 366 general increase of CD163 labelling in all the compartments (cortex, medulla and stroma) with
874
875 367 abundant intravascular CD163 positive cells. The increase in the number of CD172a and CD163
876
877 368 positive cells observed in both infected groups at 10-14 dpi was associated with the marked
878
879 369 inflammatory infiltrate of the stroma of the thymus as well as with the extensive cell death of
880
881 370 cortical thymocytes. Thus, monocytes/macrophages may be migrating from the bloodstream and
882
883 371 other tissues to the thymus through chemotaxis from inflammatory foci as well as from a high
884
885
886 372 demand of phagocytosis of cell death debris in the thymic cortex. The identification of intravascular
887
888 373 CD172a and CD163 positive cells observed in the present study supports this hypothesis.
889
890 374 Furthermore, the increase in the number of CD163 positive cells may also get along with the
891
892 375 induction of this surface molecule in resident tissue macrophages from the thymus. Interestingly,
893
894 376 the induction of CD163 has been proved in CD163 negative monocytes from bone marrow after *in*
895
896 377 *vitro* PRRSV infection (Fernández-Caballero et al.,2018) The higher frequency of CD163 positive
897
898
899
900

901
902
903 378 cells observed in both infected groups along our study may answer to different strategies of the
904
905 379 virus: (1) to increase the number of susceptible cells to virus replication (Patton et al. 2009); (2) to
906
907
908 380 allow PRRSV persistence in the thymus (Patton et al. 2009); (3) to lead to the modulation of the
909
910 381 inflammatory and immune response through the induction of haptoglobin and IL-10 (Philippidis et
911
912 382 al., 2004) or (4) to increase the phagocytic activity of macrophages through the binding of the
913
914 383 scavenger receptor to Gram-positive and Gram-negative bacteria (Fabriek et al., 2009).
915
916 384
917
918 385 CD107a immunolabelling was mainly found in the thymic cortex in the control group, while a
919
920 386 generalised decrease in the frequency of positive cells was observed in infected animals, with the
921
922 387 only exception of infected animals at 10-14 dpi, which presented a mild increase of CD107a
923
924
925 388 positive cells in the stroma. Compared with the other markers, the number of BA4D5 positive cells
926
927 389 was much lower, with an enhancement in the number of positive cells mainly in the cortex of both
928
929 390 infected groups at 10-14 dpi and in a lesser extent in the thymic medulla of vaccinated animals. The
930
931 391 decrease in the number of CD107a positive cells together with the increase in the number of
932
933 392 BA4D5 positive cells highlight different mechanisms of regulation of the cytotoxic activity not only
934
935 393 in infected pigs but also in vaccinated animals, which may be potentially involved in the
936
937 394 modulation of the host immune response. BA4D5 antibody is thought to be specific for porcine
938
939 395 CD68, which is mainly expressed by cells from the monocyte lineage, by circulating macrophages
940
941
942 396 and by tissue macrophages (Taylor et al., 2005). Among other functions CD68 plays a role in the
943
944 397 cytotoxic activity, with a predominant intracellular location in phagolysosomes (Kurushima et al.,
945
946 398 2000); phagocytic activity, associated to the scavenger receptor family and promoting cellular
947
948 399 debris clearance (Taylor et al., 2005) and mediating the recruitment and activation of macrophages
949
950 400 through binding to specific lectins and selectins (Song et al., 2011). In our study, the increase in the
951
952 401 number of perivascular and intravascular BA4D5 positive cells observed in animals from both
953
954 402 infected groups at 10-14 dpi as well as in vaccinated animals support the potential role of this
955
956 403 molecule in macrophages recruitment observed mainly in infected pigs at 10-14 dpi.
957

961
962
963 404
964
965 405 The main evidence observed in the present work was the presence of severe histopathological
966
967
968 406 lesions in the thymus of the animals infected with PR11 and PR40 PRRSV strains that died at 10-14
969
970 407 dpi, and the increase in the number of macrophages in the different compartments of the thymus.
971
972 408 The different markers used in this study allow us identifying the recruitment of macrophages
973
974 409 associated to the strong and early inflammatory response in the stroma of the thymus, the increase
975
976 410 in the expression of the major receptor of PRRSV and the regulation of the host cytotoxic activity
977
978 411 by macrophages. Interestingly, no marked differences were observed between the low virulent
979
980 412 PR11 and the virulent PR40 strains used in this study. Our results give some light to the
981
982 413 dysregulation of the host immune response by PRRSV and how the infection of the macrophage
983
984
985 414 population during the early phases of the disease may influence the decrease of the T cell
986
987 415 population, already demonstrated in other studies (Canelli et al., 2017). Finally, our results point out
988
989 416 that heterologous vaccination is a useful strategy to restrain virus spread as well as the extent of the
990
991 417 lesions observed in animals infected with virulent strains of PRRSV.
992

993 418
994
995 419 **Acknowledgements**
996

997 420 The authors would like to thank Gema Muñoz and Alberto Alcántara for their technical assistance.
998
999 421 Giulia Ogno is funded by a pre-doctoral grant of the Department of Veterinary Science, University
1000
1001 422 of Parma, Italy. Dr. Elena Canelli was funded by grants of the Department of Veterinary Science,
1002
1003
1004 423 University of Parma. J. Gómez-Laguna is supported by a “Ramón y Cajal” contract of the Spanish
1005
1006 424 Ministry of Economy and Competitiveness (RYC-2014-16735). This work was partially supported
1007
1008 425 by the Spanish Ministry of Education and Science (Grant #AGL2016-76111-R).
1009

1010 426
1011
1012 427 **References**
1013

1014 428 Adams, M.J., Lefkowitz, E.J., King, A.M.Q., Harrach, B., Harrison, R.L., Knowles, N.J., Kropi
1015
1016 429 nski, A.M., Krupovic, M., Kuhn, J.H., Mushegian, A.R., Nibert, M., Sabanadzovic, S., Sa

1021
1022
1023 430 nfaçon, H., Siddell, S.G., Simmonds, P., Varsani, A., Zerbini, F.M., Gorbalenya, A.E., D
1024
1025 431 avison, A.J., 2017. Changes to taxonomy and the international code of virus
1026
1027 432 classification and nomenclature ratified by the International Committee on Taxonomy of
1028
1029 Viruses. Arch Virol. 162, 2505–2538. doi:10.1007/s00705-017-3358-5.
1030 433
1031
1032 434 Amarilla, S.P., Gómez-Laguna, J., Carrasco, L., Rodríguez-Gómez, I.M., Caridad, Y.O.J.M.,
1033
1034 435 Graham, S.P., Frossard, J.P., Steinbach, F., Salguero, F.J., 2016. Thymic depletion of
1035
1036 436 lymphocytes is associated with the virulence of PRRSV-1 strains. Vet. Microbiol. 188,
1037
1038 437 47-58. <https://doi.10.1016/j.vetmic.2016.04.005>.
1039
1040 438 Álvarez, B., Sánchez, C., Bullido, R., Marina, A., Lunney, J., Alonso, F., Ezquerra, A.,
1041
1042 439 Domínguez, J., 2000. A porcine cell surface receptor identified by monoclonal
1043
1044 440 antibodies to SWC3 is a member of the signal regulatory protein family and associates
1045
1046 441 with protein- tyrosine phosphatase SHP-1. Tissue Antigens 55, 342–351.
1047
1048 442 Aktas, E., Kucuksezer, U.C., Bilgic, S., Erten, G., Deniz, G., 2008. Relationship between
1049
1050 443 CD107a expression and cytotoxic activity. Cell Immunol. 254, 149–154. doi:
1051
1052 444 10.1016/j.cel- limm.2008.08.007 PMID:18835598. ☒
1053
1054 445 Balka, G., Podgórska, K., Brar, M.S., Bálint, Á., Cadar, D., Celer, V., Dénes, L., Dirbakova, Z.,
1055
1056 446 Jedryczko, A., Márton, L., Novosel, D., Petrović, T., Sirakov, I., Szalay, D., Toplak, I.,
1057
1058 447 Leung, F.C., Stadejek, T., 2018. Genetic diversity of PRRSV 1 in Central Eastern
1059
1060 448 Europe in 1994-2014: origin and evolution of the virus in the region. Sci Rep. 8, 7811.
1061
1062 449 doi: 10.1038/s41598-018-26036-w.
1063
1064 450 Barranco, I., Gómez-Laguna, J., Rodríguez-Gómez, I.M., Quereda, J.J., Salguero, F.J., Pallarés,
1065
1066 451 F.J., Carrasco, L., 2012. Immunohistochemical expression of IL-12, IL-10, IFN-alpha
1067
1068 452 and IFN-gamma in lymphoid organs of porcine reproductive and respiratory syndrome
1069
1070 453 virus-infected pigs. Vet. Immunol. Immunopathol. 149, 262–271.
1071
1072 454 <https://doi.10.1016/j.vetimm.2012.07.011>.
1073
1074
1075
1076
1077
1078
1079
1080

- 1081
1082
1083
1084 455 Bonckaert, C., Van der Meulen, K., Rodriguez-Ballara, I., Sanz, P., Fenech Martinez, P.,
1085 456 Nauwynck, H., 2016. Modified-live PRRSV subtype 1 vaccine UNISTRAIN PRRS
1086 provides a partial clinical and virological protection upon challenge with East European
1087 subtype 3 PRRSV strain Lena. P.H.M. 2, 12. doi: 10.1186/s40813-016-0029-y.
1088 457
1089
1090 458
1091
1092 459 Bullido, R., Gomez del Moral, M., Alonso, F., Ezquerra, A., Zapata, A., Sánchez, C., et
1093 al.,1997. Monoclonal antibodies specific for porcine monocytes/macrophages:
1094 460 macrophage heterogeneity in the pig evidenced by the expression of surface antigens.
1095 Tissue Antigens. 49, 403–13. <https://doi.org/10.1111/j.1399-0039.1997.tb02769.x>
1096 461
1097
1098 462
1099
1100 463 Burkard, C, Lillico, S.G., Reid, E., Jackson, B., Mileham, A.J., Ait-Ali, T., Whitelaw,
1101 C.B.A., Archibald, A.L.,2017. Precision engineering for PRRSV resistance in pigs:
1102 464 Macrophages from genome edited pigs lacking CD163 SRCR5 domain are fully resistant
1103 to both PRRSV genotypes while maintaining biological function. Plos pathogens.
1104 465 13(2):e1006206 <https://doi.org/10.1371/journal.ppat.1006206>.
1105
1106 466
1107
1108
1109 467
1110
1111 468 Butler, J.E., Lager, K.M., Golde, W., Faaberg, K.S., Sinkora, M., Loving, C., Zhang, Y.I., 2014.
1112 Porcine reproductive and respiratory syndrome (PRRS): An immune dysregulatory
1113 469 pandemic. Immunol. Res. 59, 81–108. <https://doi.10.1007/s12026-014-8549-5>.
1114
1115 470
1116
1117 471 Calvert, J.G., Slade, D.E., Shields, S.L., Jolie, R., Mannan, R.M., Ankenbauer, R.G., Welch,
1118 S.K, 2007. CD163 expression confers susceptibility to porcine reproductive and
1119 472 respiratory syndrome viruses. J Virol. 81,7371–9.
1120
1121
1122 473
1123
1124 474 Canelli, E., Catella, A., Borghetti, P., Ferrari, L., Ogno, G., De Angelis, E., Corradi, A., Passeri,
1125 B., Bertani, V., Sandri, G., Bonilauri, P., Leung, F.C., Guazzetti, S., Martelli, P., 2017.
1126 475 Phenotypic characterization of a highly pathogenic Italian porcine reproductive and
1127 respiratory syndrome virus (PRRSV) type 1 subtype 1 isolate in experimentally infected
1128 476 pigs. Vet Microbiol. 210, 124-133. <http://dx.doi.org/10.1016/j.vetmic.2017.09.002>.
1129
1130 477
1131
1132 478
1133
1134 479 Canelli, E., Catella, A., Borghetti, P., Ferrari, L., Ogno, G., Corradi, A., De Angelis, E.,
1135 Bonilauri, P., Guazzetti, S., Martelli, P., 2018. Evaluation of the efficacy of a
1136 480

- 1141
1142
1143
1144 481 commercial modified live virus vaccine against a highly pathogenic Italian PRRSV-1 in
1145
1146 482 experimentally infected pigs. *Veterinary Microbiology*. 226, 89-96.
1147
1148 483 <https://doi.10.1016/j.vetmic.2018.10.001>.
- 1149
1150 484 Do, D.T., Park, C., Choi, K., Jeong, J., Nguyen, T.T., Nguyen, K.D., Chae, C., 2015.
1151
1152 485 Comparison of two genetically distant type 2 porcine reproductive and respiratory
1153
1154 486 syndrome virus (PRRSV) modified live vaccines against Vietnamese highly pathogenic
1155
1156 487 PRRSV. *Vet. Microbiol.* 179, 233-241. doi: 10.1016/j.vetmic.2015.06.013.
- 1158
1159 488 Domenech, N., Rodriguez-Carreno, M.P., Filgueira, P., Alvarez, B., Chamorro, S., Domínguez,
1160
1161 489 J., 2003. Identification of porcine macrophages with monoclonal antibodies in formalin-
1162
1163 490 fixed, paraffin-embedded tissues. *Vet Immunol Immunopathol.* 94, 77–81.
1164
1165 491 [https://doi.org/10.1016/s0165-2427\(03\)00084-9](https://doi.org/10.1016/s0165-2427(03)00084-9).
- 1166
1167 492 Duan, X., Nauwynck, H.J., Pensaert, M.B., 1997. Virus quantification and identification of
1168
1169 493 cellular targets in the lungs and lymphoid tissues of pigs at different time intervals after
1170
1171 494 inoculation with porcine reproductive and respiratory syndrome virus (PRRSV). *Vet*
1172
1173 495 *Microbiol.* 56, 9–19. [https://doi.org/10.1016/S0378-1135\(96\)01347-8](https://doi.org/10.1016/S0378-1135(96)01347-8).
- 1174
1175 496 Ezquerra, A., Revilla, C., Alvarez, B., Perez, C., Alonso, F., Dominguez, J., 2009. Porcine
1176
1177 497 myelomonocytic markers and cell populations. *Dev. Comp. Immunol.* 33, 284-298.
1178
1179 498 <https://doi.org/10.1016/j.dci.2008.06.002>.
- 1180
1181 499 Fabrick, B. O., van Bruggen, R., Deng, D. M., et al., 2009. The macrophage scavenger receptor
1182
1183 500 CD163 functions as an innate immune sensor for bacteria. *Blood*. 113, no. 4, pp. 887–
1184
1185 501 892. ☒
- 1186
1187
1188 502 Frydas, I.S., Trus, I., Kvisgaard, L.K., Bonckaert, C., Reddy, V.R., Li, Y., Larsen, L.E.,
1189
1190 503 Nauwynck, H.J., 2015. Different clinical, virological, serological and tissue tropism
1191
1192 504 outcomes of two new and one old Belgian type 1 subtype 1 porcine reproductive and
1193
1194
1195
1196
1197
1198
1199
1200

- 1201
1202
1203
1204
1205
1206
1207
1208
1209
1210
1211
1212
1213
1214
1215
1216
1217
1218
1219
1220
1221
1222
1223
1224
1225
1226
1227
1228
1229
1230
1231
1232
1233
1234
1235
1236
1237
1238
1239
1240
1241
1242
1243
1244
1245
1246
1247
1248
1249
1250
1251
1252
1253
1254
1255
1256
1257
1258
1259
1260
- respiratory virus (PRRSV) isolates. *Vet Res* 46, 37. [https://doi: 10.1186/s13567-015-0166-3](https://doi.org/10.1186/s13567-015-0166-3)
- Geissmann, F., Gordon, S., Hume, D.A., Mowat, A.M., Randolph, G.J., 2010. Unravelling mononuclear phagocyte heterogeneity. *Nat Rev Immunol.* 10, 453–460. doi: 10.1038/nri2784.
- Gómez-Laguna, J., Salguero, F.J., Barranco, I., Pallarés, F.J., Rodríguez-Gómez, I.M., Bernabé, A., Carrasco, L., 2010. Cytokine expression by macrophages in the lung of pigs infected with the porcine reproductive and respiratory syndrome virus. *J. Comp. Pathol.* 142, 51–60. <https://doi.org/10.1016/j.jcpa.2009.07.004>.
- Gómez-Laguna, J., Salguero, F.J., Pallarés, F.J., Carrasco, L., 2013. Immunopathogenesis of porcine reproductive and respiratory syndrome in the respiratory tract of pigs. *Vet. J.* 195, 148–155. <https://doi.org/10.1016/j.tvjl.2012.11.012>.
- Gorbalenya, A.E., Krupovic, M., Siddell, S., Varsani, A., Kuhn, J.H., 2018. Riboviria: establishing a single taxon that comprises RNA viruses at the basal rank of virus taxonomy. *International Committee on Taxonomy of Viruses: https://talk.ictvonline.org/taxonomy/p/taxonomy-history?taxnode_id=20186087*
- Han, J., Zhou, L., Ge, X., Guo, X. & Yang, H., 2017. Pathogenesis and control of the Chinese highly pathogenic porcine reproductive and respiratory syndrome virus. *Veterinary microbiology.* 209, 30–47. <https://doi.org/10.1016/j.vetmic.2017.02.020>.
- He, Y., Wang, G., Liu, Y., Shi, W., Han, Z., Wu, J., Jiang, C., Wang, S., Hu, S., Wen, H., Dong, J., Liu, H., Cai, X., 2012. Characterization of thymus atrophy in piglets infected with highly pathogenic porcine reproductive and respiratory syndrome virus. *Vet. Microbiol.* 160, 455–462. <https://doi.org/10.1016/j.vetmic.2012.05.040>.
- Karniychuk, U.U., M. Geldhof, M. Vanhee, J. Van Doorselaere, T.A., Saveleva, Nauwynck, H. J., 2010. Pathogenesis and antigenic characterization of a new East European subtype 3

- 1261
1262
1263
1264 331 porcine reproductive and respiratory syndrome virus isolate. BMC Vet. Res. 6, 30.
1265
1266 332 <https://doi.org/10.1186/1746-6148-6-30>.
- 1267
1268 333 Kurushima, H., Ramprasad, M., Kondratenko, N., Foster, D.M., Quehenberger, O., Steinberg
1269
1270 334 D., 2000. Surface expression and rapid internalization of macrosialin (mouse CD68) on
1271
1272 335 elicited mouse peritoneal macrophages. J. Leukoc. Biol. 67, 104–108.
1273
1274 336 <https://doi.org/10.1002/jlb.67.1.104>.
- 1275
1276 337 Law, S.K.A., Micklem, K.J., Shaw, J.M., Zhang, X.P., Dong, Y., Willis, A.C., Mason, , D.Y.,
1277
1278 338 1993. A new macrophage differentiation antigen which is a member of the scavenger
1279
1280 339 receptor superfamily. Eur. J. Immunol. 23, 2320–5.
1281
1282 340 <https://doi.org/10.1002/eji.1830230940>.
- 1283
1284 341 Lunney, J.K., Benfield, D.A., Rowland, R.R., 2010. Porcine reproductive and respiratory
1285
1286 342 syndrome virus: an update on an emerging and re-emerging viral disease of swine. Virus
1287
1288 343 Res. 154, 1–6. <https://doi.org/10.1016/j.virusres.2010.10.009>.
- 1289
1290 344 Morgan, S.B., Graham, S.P., Salguero, F.J., Sánchez-Cordón, P.J., Mokhtar, H., Rebel, J.M.J.,
1291
1292 345 Weesendorp, E., Bodman-Smith, K.B., Steinbach, F., Frossard, J.P., 2013. Increased
1293
1294 346 pathogenicity of European porcine reproductive and respiratory syndrome virus is
1295
1296 347 associated with enhanced adaptive responses and viral clearance. Vet Microbiol 163, 13-
1297
1298 348 22. <https://doi:10.1016/j.vetmic.2012.11.024>.
- 1299
1300 349 Murtaugh, M.P., Stadejek, T., Abrahante, J.E., Lam, T.T., Leung, F.C., 2010. The ever-
1301
1302 350 expanding diversity of porcine reproductive and respiratory syndrome virus. Virus
1303
1304 351 Res. 154, 18-30. <https://doi.org/10.1016/j.virusres.2010.08.015>.
- 1305
1306 352 Nelsen, C. J., Murtaugh, M.P., Faaberg, K.S., 1999. Porcine reproductive and respiratory
1307
1308 353 syndrome virus comparison: divergent evolution on two continents. J Virol 73(1): 270-
1309
1310 354 280.
- 1311
1312 355 Patton, J.B., Rowland, R.R., Yoo, D., Chang, K.O., 2009. Modulation of CD163 receptor
1313
1314 356 expression and replication of porcine reproductive and respiratory syndrome virus in
1315
1316
1317
1318
1319
1320

1321
1322
1323
1324 57 porcine macrophages. *Virus Research*, vol. 140, no. 1-2, pp. 161–171, 2009.
1325
1326 58 <https://doi.org/10.1016/j.virusres.2008.12.002>.
1327
1328 59 Pearse, G., 2006a. Histopathology of the thymus. *Toxicol. Pathol.* 34, 515–547.
1329
1330 60 Pearse, G., 2006b. Normal structure, function and histology of the thymus. *Toxicol. Pathol.* 34,
1331
1332 61 504–514.
1333
1334 62 Perez, C., Ortuno, E., Gomez, N., Garcia-Briones, M., Alvarez, B., Martinez de la Riva, P.,
1335
1336 63 Alonso, F., Revilla, C., Domínguez, J., Ezquerro, A., 2008. Cloning and expression of
1337
1338 64 porcine CD163: its use for characterization of monoclonal antibodies to porcine CD163
1339
1340 65 and development of an ELISA to measure soluble CD163 in biological fluids. *Span J*
1341
1342 66 *Agric Res.* 6, 59–72. <https://doi.10.5424/sjar/200806S1-374>.
1343
1344 67 Philippidis, P., Mason, J.C., Evans, B.J., Nadra, I., Taylor, K.M., Haskard, D.O., Landlis, R.C.,
1345
1346 68 2004. Hemoglobin scavenger receptor CD163 mediates inter- leukin-10 release and
1347
1348 69 heme oxygenase-1 synthesis: anti-inflammatory monocyte-macrophage responses in
1349
1350 70 *in vitro*, in resolving skin blisters *in vivo*, and after cardiopulmonary bypass surgery. *Circ*
1351
1352 71 *Res* 94, 119-126. <https://doi.10.1161/01.RES.0000109414.78907.F9>.
1353
1354 72 Rodríguez-Gómez, I.M., Gómez-Laguna, J., Carrasco, L., 2013. Impact of PRRSV on activation
1355
1356 73 and viability of antigen presenting cells. *World J. Virol.* 2, 146–151.
1357
1358 74 <https://doi.10.5501/wjv.v2.i4.146>.
1359
1360 75 Sánchez, C., Domenech, N., Vázquez, J., Alonso, F., Ezquerro, A., Domínguez, J., 1999. The
1361
1362 76 porcine 2A10 antigen is homologous to human CD163 and related to macrophage
1363
1364 77 differentiation. *J Immunol.* 162, 5230–5237.
1365
1366 78 Sinn, L.J., Klingler, E., Lamp, B., Brunthaler, R., Weissenböck, H., Rumenapf, T., Ladinig, A.,
1367
1368 79 2016. Emergence of a virulent porcine reproductive and respiratory syndrome virus
1369
1370 80 (PRRSV) 1 strain in Lower Austria. *Porcine Health Manag* 2,
1371
1372 81 28. [https://doi: 10.1186/s40813-016-0044-z](https://doi:10.1186/s40813-016-0044-z)
1373
1374
1375
1376
1377
1378
1379
1380

- 1381
1382
1383
1384 582 Song, L., Lee, C., & Schindler, C., 2011. Deletion of the murine scavenger receptor
1385 CD68. *Journal of Lipid Research*, 52(8), 1542–1550. <https://doi.10.1194/jlr.m015412>.
1386
- 1387
1388 584 Stadejek, T., Oleksiewicz, M.B., Scherbakov, A.V., Timina, A.M., Krabbe, J.S., Chabros, K.,
1389 Potapchuk, D., 2008. Definition of subtypes in the European genotype of porcine
1390 585 reproductive and respiratory syndrome virus: nucleocapsid characteristics and
1391 geographical distribution in Europe. *Arch Virol* 153, 1479-1488.
1392
1393
1394 587
1395
1396 588
1397
1398 589 Stadejek, T., Stankevicius, A., Murtaugh, M.P., Oleksiewicz, M.B., 2013. Molecular evolution
1399 of PRRSV in Europe: current state of play. *Vet Microbiol* 165, 21-28.
1400
1401
1402 590
1403
1404 591
1405 592 Stadejek, T., Larsen, L.E., Podgórska, K., Botner, A., Botti, S., Dolka, I., Fabisiak, M.,
1406 Heegaard, P.M.H., Hjulsager, C.K., Huc, T., Kvisgaard, L.K., Sapierzynski, R., Nielsen,
1407 593 J., 2017. Pathogenicity of three genetically diverse strains of PRRSV Type 1 in specific
1408 pathogen free pigs. *Vet Microbiol* 209,13-19. [https://doi: 10.1016/j.vetmic.2017.05.011](https://doi:10.1016/j.vetmic.2017.05.011).
1409 594
1410
1411 595
1412
1413 596 Summerfield, A., McCullough, K.C., 1997. Porcine bone marrow myeloid cells: phenotype and
1414 adhesion molecule expression. *J Leukoc Biol.* 62, 176–85.
1415 597
1416
1417 598
1418
1419 599 Taylor, P.R., Martinez-Pomares, L., Stacey, M., Lin, H.H., Brown, G.D., Gordon, S., 2005.
1420
1421 600
1422
1423
1424 601
1425
1426 602 Tian, K., Yu, X., Zhao, T., Feng, Y., Cao, Z., Wang, C., Hu, Y., Chen, X., Hu, D., Tian, X., Liu,
1427 D., Zhang, S., Deng, X., Ding, Y., Yang, L., Zhang, Y., Xiao, H., Qiao, M., Wang, B.,
1428 603 Hou, L., Wang, X., Yang, X., Kang, L., Sun, M., Jin, P., Wang, S., Kitamura, Y., Yan,
1429 J., Gao, G.F., 2007. Emergence of fatal PRRSV variants: unparalleled outbreaks of
1430 604 atypical PRRS in China and molecular dissection of the unique hallmark. *PLoS One*
1431
1432 605
1433
1434
1435 606
1436
1437
1438
1439
1440

1441
1442
1443
1444
1445
1446
1447
1448
1449
1450
1451
1452
1453
1454
1455
1456
1457
1458
1459
1460
1461
1462
1463
1464
1465
1466
1467
1468
1469
1470
1471
1472
1473
1474
1475
1476
1477
1478
1479
1480
1481
1482
1483
1484
1485
1486
1487
1488
1489
1490
1491
1492
1493
1494
1495
1496
1497
1498
1499
1500

2:e526. <https://doi.10.1371/journal.pone.0000526>.

- Trus, I., Bonckaert, C., van der Meulen, K., Nauwynck, H.J., 2014. Efficacy of an attenuated European subtype 1 porcine reproductive and respiratory syndrome virus (PRRSV) vaccine in pigs upon challenge with the East European subtype 3 PRRSV strain Lena. *Vaccine* 32, 2995-3003. doi: 10.1016/j.vaccine.2014.03.077.
- Van Breedam, W., Delputte, P. L., Van Gorp, H., Misinzo, G., Vanderheijden, N., Duan, X., Nauwynck, H.J., 2010. Porcine reproductive and respiratory syndrome virus entry into the porcine macrophage. *Journal of General Virology* 91(7): 1659-1667. <https://doi.10.1099/vir.0.020503-0>.
- Whitworth KM, Rowland, R.R., Ewen, C.L., Tribble, B.R., Kerrigan, M.A., Cino-Ozuna, A.G., Samuel, M.S., Lightner, J.E., McLaren, D.G., Mileham, A.J., Wells, K.D., Prather, R.S., 2016. Gene-edited pigs are protected from porcine reproductive and respiratory syndrome virus. *Nature Biotechnology*. 34: 20–22. doi: 10.1038/nbt.3434.

1501
1502
1503
1504
1505
1506
1507
1508
1509
1510
1511
1512
1513
1514
1515
1516
1517
1518
1519
1520
1521
1522
1523
1524
1525
1526
1527
1528
1529
1530
1531
1532
1533
1534
1535
1536
1537
1538
1539
1540
1541
1542
1543
1544
1545
1546
1547
1548
1549
1550
1551
1552
1553
1554
1555
1556
1557
1558
1559
1560

Figure captions

Fig. 1. Experimental design

Fig. 2. Representative photomicrographs of the thymus from a control pig (A; Haematoxylin-eosin, HE; Bar, 100 μ m), a PR11-infected pig dead at 10-14 dpi with a strong disappearance of the corticomedullary boundary (B; HE; Bar, 100 μ m; Hassall's corpuscles are identified with two black arrows), and a PR40-infected pig dead at 10-14 dpi with a marked interstitial inflammatory infiltrate of the stroma by abundant neutrophils and mononuclear cells (macrophages, lymphocytes and plasma cells in a lesser extent) particularly intense at perivascular level is showed (C; HE; Bar, 100 μ m; a Hassall's corpuscle is identified with an asterisk). A higher magnification of the perivascular infiltrate, highlighted with a black dashed line in C, is showed (D; HE; Bar, 50 μ m).

Fig. 3. (A) Counts for PRRSV N protein positive cells in the thymic cortex (blue column), medulla (red column), stroma (green column) and total (the empty circles represent individual values; the mean is showed as a black solid line). (B) N protein positive cells (arrows) in the thymic cortex of a PR11-infected pig that died at 10-14 dpi (IHC, Bar, 50 μ m). (C) High number of N protein positive cells in the stroma and in the thymic cortex of a PR40-infected pig that died at 10-14 dpi (IHC, Bar, 50 μ m). *Inset*, detail of the cytoplasmic staining against PRRSV N protein in a macrophage from the stroma of a PR40-infected pig that died at 10-14 dpi (IHC, Bar, 20 μ m). (D) TUNEL labelling of tingible body macrophages in the cortex of the thymus of a control animal (TUNEL, Bar, 50 μ m). (E) Marked increase of TUNEL labelling in the cortex of a PR11-infected animal at 10-14 dpi, with a diffuse labelling associated to an intense increase of cell death (TUNEL, Bar, 50 μ m).

Fig. 4. Counts for CD172a (A) and CD163 (B) positive cells in the thymic cortex (blue column), medulla (red column), stroma (green column) and total (the empty circles represent individual values; the mean is showed as a black solid line). (C) CD172a positive cells in the thymic medulla of a PR40-infected animal and killed at 35 dpi (IHC, Bar, 50 μ m). (D) An increased number of CD172a positive cells in the stroma and the cortex of the thymus from a PR11-infected animal that died at 10-14 dpi (IHC, Bar, 50 μ m). *Inset*, detail of the cytoplasmic staining against CD172a in

1561
1562
1563
1564 646 several macrophages from the stroma of a PR11-infected pig that died at 10-14 dpi (IHC, Bar,
1565
1566 647 20µm). (E) Scattered CD163 positive cells in the cortex and medulla of the thymus from a PR11-
1567
1568 648 infected animal that died at 10-14 dpi (IHC, Bar, 50µm). (F) Numerous macrophages and tingible
1569
1570 649 body macrophages within the thymic cortex and stroma of a PR40-infected pig at 10-14 dpi (IHC,
1571
1572 650 Bar, 50µm). *Inset*, detail of the cytoplasmic staining against CD163 in macrophages from the
1573
1574 651 stroma of a PR40-infected pig at 10-14 dpi (IHC, Bar, 20µm).

1575
1576 652 **Fig. 5.** Counts for CD107a (A) and BA4D5 (B) positive cells in the thymic cortex (blue column),
1577
1578 653 medulla (red column), stroma (green column) and total (the empty circles represent individual
1579
1580 654 values; the mean is showed as a black solid line). (C) Numerous tingible body macrophages
1581
1582 655 immunolabelled against CD107a in the thymic cortex of a control animal at 35 dpi (IHC, Bar,
1583
1584 656 20µm). *Inset*, detail of the cytoplasmic staining against CD107a in a macrophage with cytoplasmic
1585
1586 657 prolongations in the thymic cortex from the same animal (IHC, Bar, 20µm). (D) Scattered CD107a
1587
1588 658 positive cells in the cortex and medulla of the thymus from a PR40-infected animal that died at 10-
1589
1590 659 14 dpi (IHC, Bar, 20µm). (E) BA4D5 positive cells in the medulla and at perivascular level in the
1591
1592 660 thymus from a VAC-PR40 animal at the end of the study (IHC, Bar, 20µm). (F) Higher
1593
1594 661 magnification of another field of the thymus from the same animal with a marked perivascular
1595
1596 662 infiltrate by BA4D5 positive cells (IHC, Bar, 20µm).

Table 1. Clones, sources and dilutions of the primary antibodies used for the immunohistochemical detection of macrophages markers.

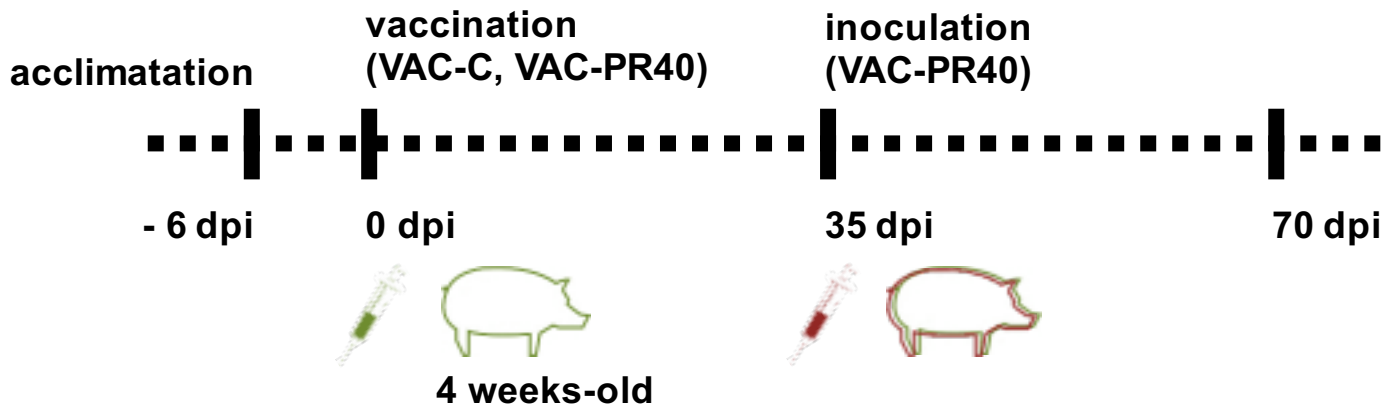
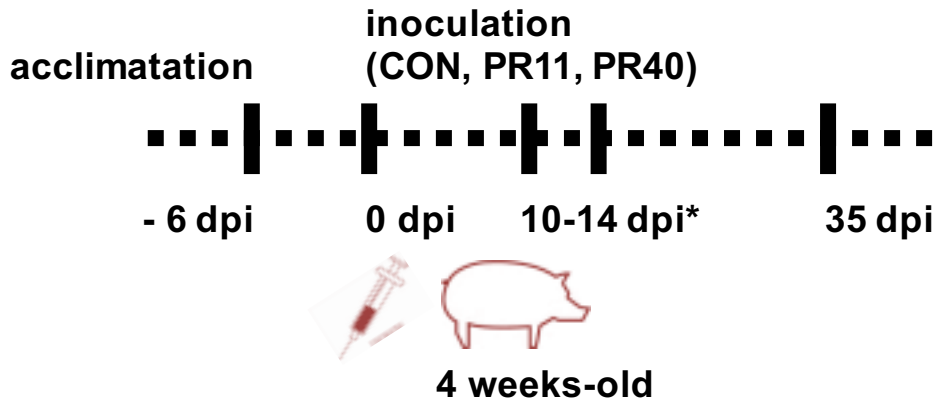
Specificity (clone)	Type of antibody	Commercial origin	Fixative	Blocking solution	Dilution	Antigen retrieval
Anti-PRRSV (clone SDOW17)	mAb	Rural Technologies Inc., Brookings, SD, USA	Formalin	BSA 1%	1:500	Protease Type XIV ^a
TUNEL	N.A.	Roche Diagnostics, Indianapolis, USA	Formalin	N.A.	N.A.	Proteinase K ^b
Anti-CD172a (BA1C11)	mAb	In house, INIA	Formalin	BSA 1%	Neat	Citrate pH 3.2
Anti-CD163 (2A10/11)	mAb	In house, INIA	Formalin	BSA 1%	Neat	Citrate pH 3.2
Anti-CD107a (4E9/11)	mAb	In house, INIA	Formalin	BSA 1%	Neat	Citrate pH 3.2
Anti-BA4D5 (BA4D5)	mAb	In house, INIA	Formalin	BSA 1%	Neat	Citrate pH 3.2

N.A.: Not applicable; ^aProtease Type XIV (Sigma-Aldrich): 8 min at 37 °C in water bath; ^bProteinase K (Roche): 15 min at 37 °C in heat incubator.

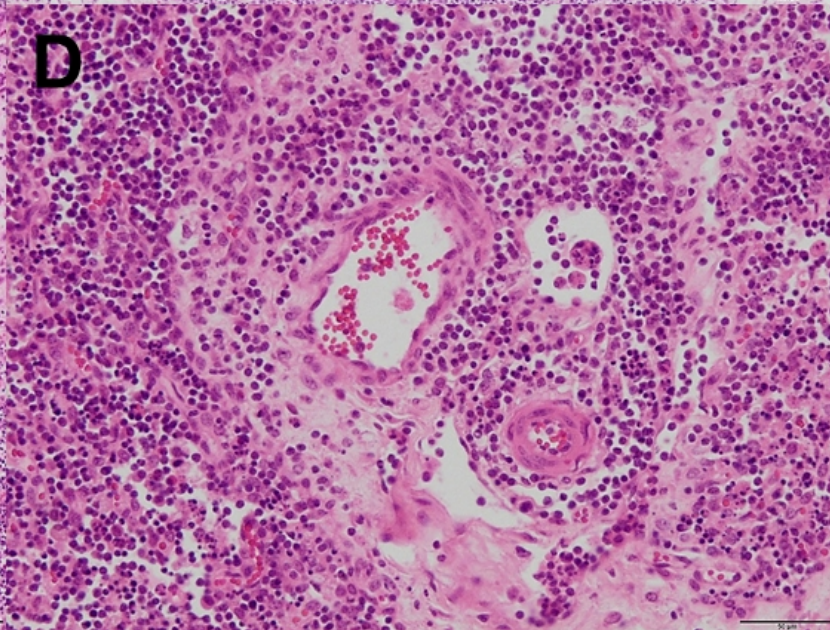
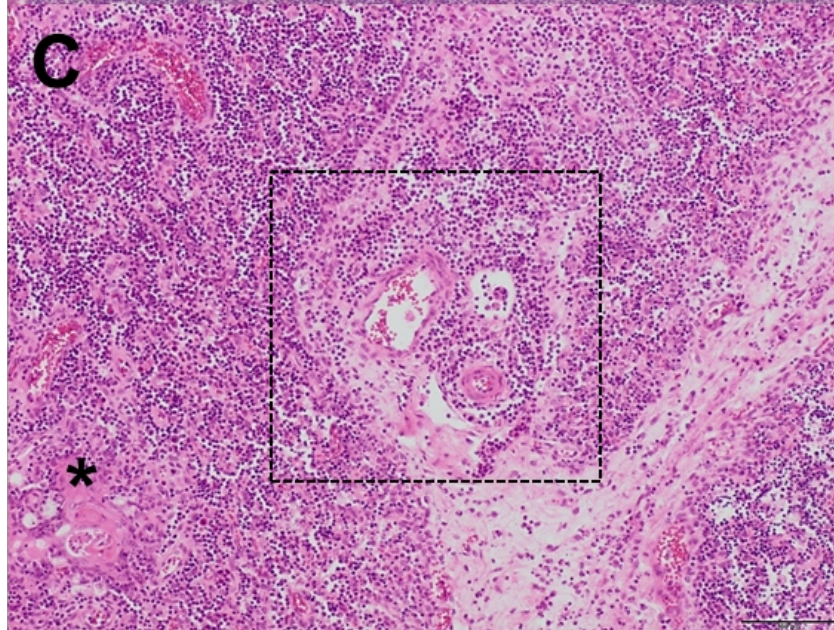
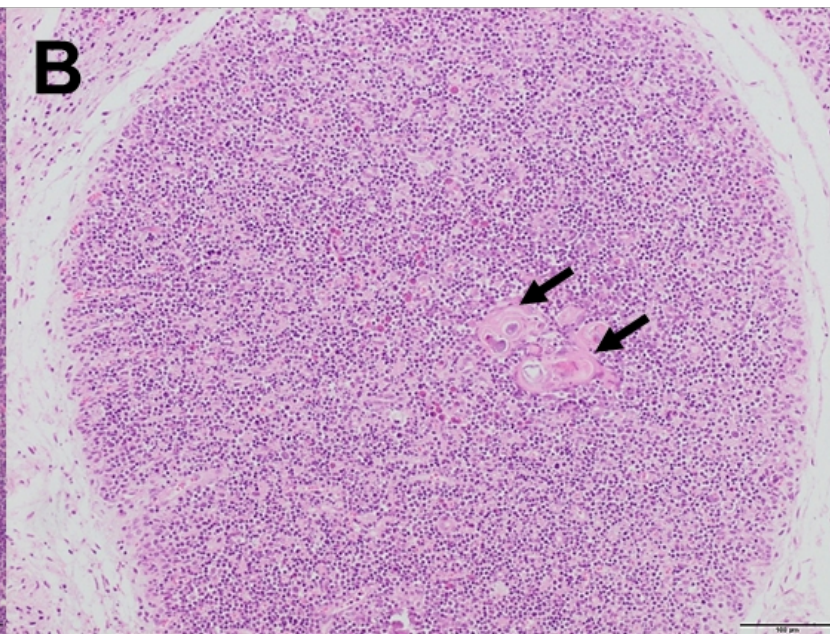
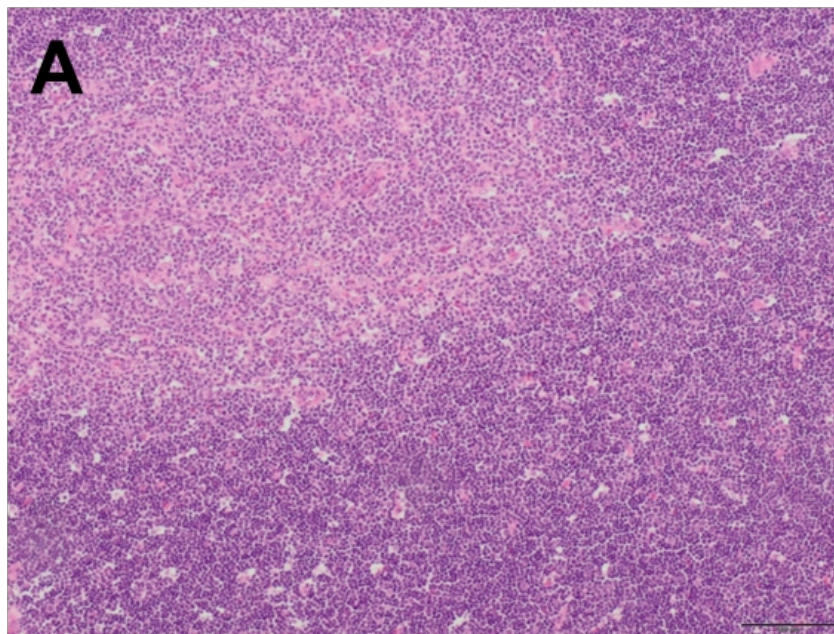
Table 2. Histopathology grading of the thymus of piglets from each experimental group and average number of tingible body macrophages and TUNEL positive cells (expressed as the mean \pm SD).

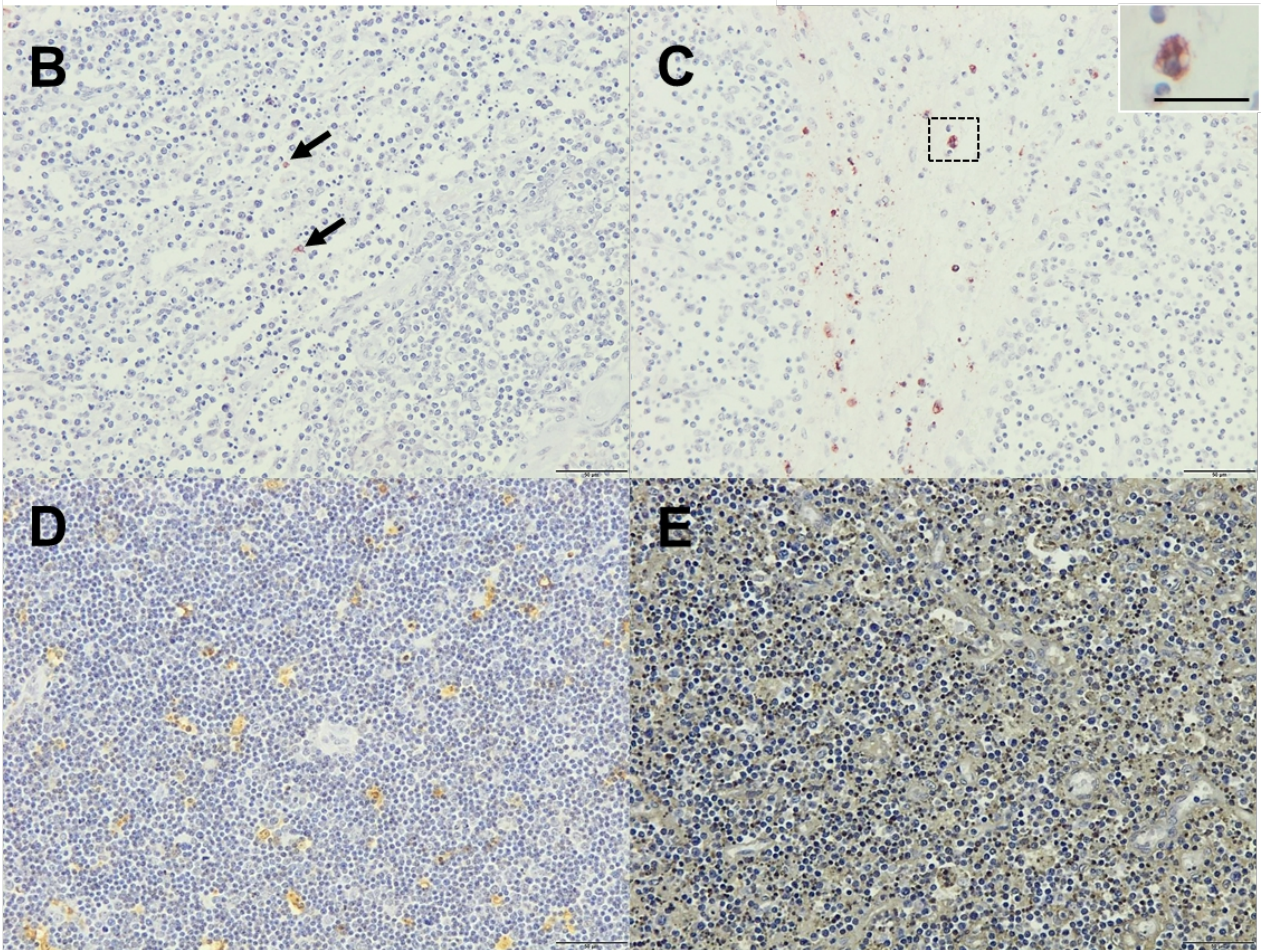
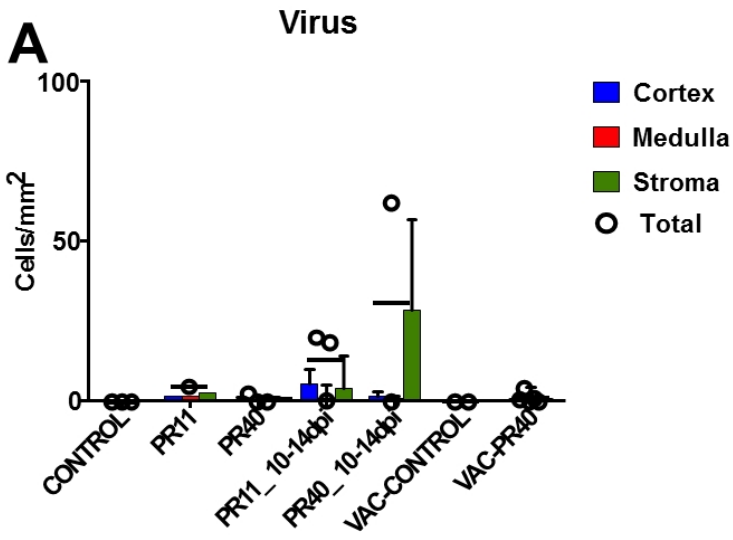
	CON (35 dpi)	PR11 (35 dpi)	PR40 (35 dpi)	PR11 (10-14 dpi)	PR40 (10-14 dpi)	VAC-C	VAC-PR40
Grades							
0	2/3	-	1/3	-	-	-	3/5
I	-	-	-	-	-	-	1/5
II	1/3	1/1	2/3	-	-	2/2	1/5
III	-	-	-	-	-	-	-
IV	-	-	-	3/3	2/2	-	-
Tingible body macrophages	9.87 \pm 1.79	7	8.87 \pm 6.82	ND*	ND*	13.1 \pm 8.63	10.4 \pm 1.79
TUNEL positive cells	54.97 \pm 63.40	67.91	43.53 \pm 31.07	ND*	ND*	53.82 \pm 40.20	53.18 \pm 34.59

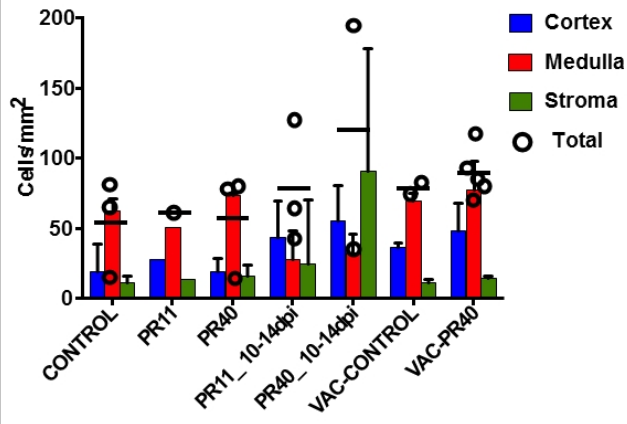
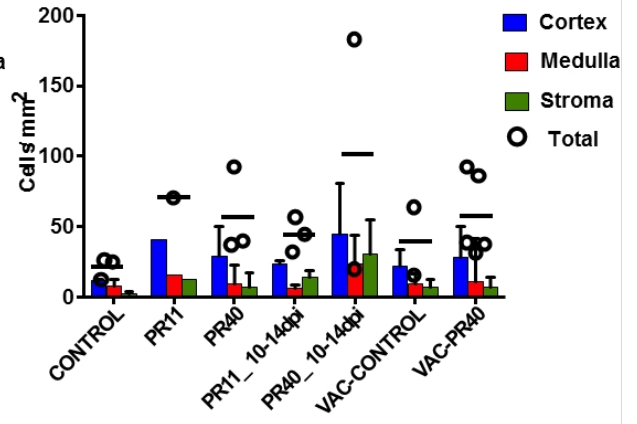
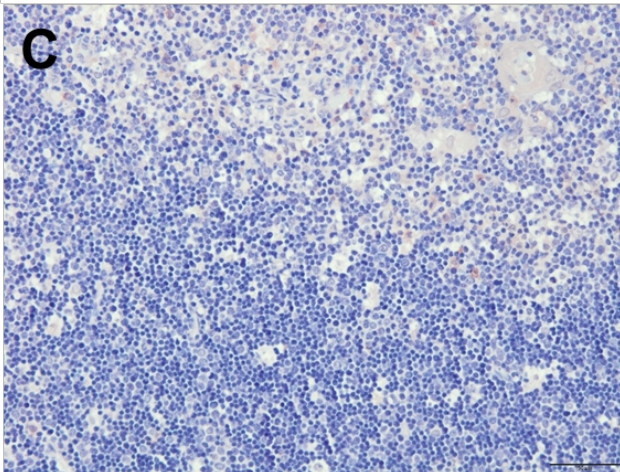
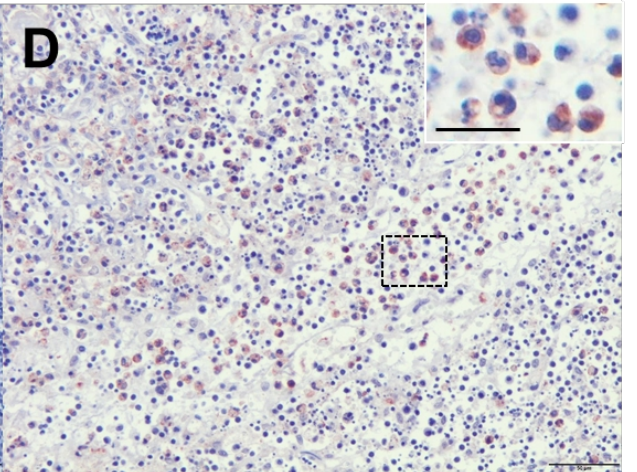
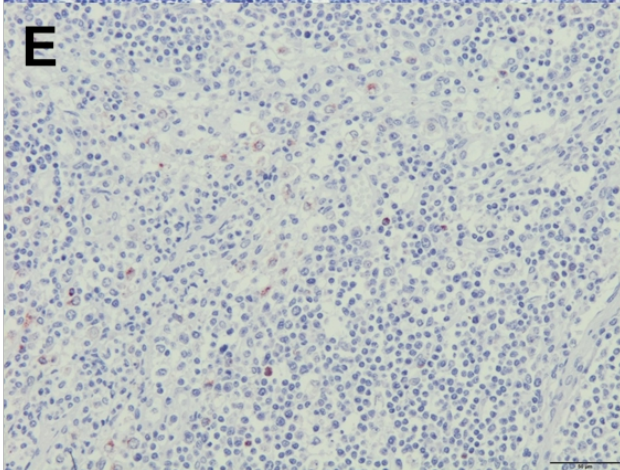
ND*: Not determined due to extensive cell death of thymocytes in the cortex.



***humanely killing of animals due to animal welfare issues**





A**CD172a****B****CD163****C****D****E****F**